Aus der Abteilung für Klinische Pharmakologie

Leiter: Prof. Dr. Stefan Endres

Medizinische Klinik und Poliklinik IV

Klinik der Universität München

Direktor: Prof. Dr. M. Reincke

Therapeutic RIG-I activation enhances survival and induces sensitivity to immune checkpoint blockade therapy in preclinical models of AML

Dissertation

zum Erwerb des Doktorgrades der Medizin

an der Medizinischen Fakultät der Ludwig-

Maximilians-Universität zu München

vorgelegt von

Michael Ruzicka

aus München

2023

Mit Genehmigung der Medizinischen Fakultät

der Universität München

1. Berichterstatter:	Prof. Dr. Simon Rothenfußer
Mitberichterstatter:	PD Dr. Hanna-Mari Baldauf
	Prof. Dr. Christian Ries
	Prof. Dr. Oliver Weigert
Mitbetreuung durch die promovierten Mitarbeiter:	Dr. Lars König
	Dr. Felix Lichtenegger
	Prof. Dr. Marion Subklewe
Dekan:	Prof. Dr. med. Thomas Gudermann
Tag der mündlichen Prüfung:	23.03.2023

Widmung:
Meinen Eltern,
meiner Tante Miluš
und meinem Cousin Přemek

Table of Contents

1. Introduction

Acute myeloid leukemia (AML) is a malignant hematologic disease deriving from primitive precursor cells of the bone marrow. Current treatment options are limited and involve serious complications, failing to achieve a cure rate higher than 5-15% in patients older than 60 years (Dohner et al. 2010, Eisfeld et al. 2018). New treatment strategies currently assessed in clinical trials involve promising immunotherapeutic approaches such as chimeric antigen receptor (CAR) T cells, the application of which is yet restricted to relapsed and/or refractory disease in most cases (Lichtenegger et al. 2017). In this work I investigated the therapeutic potential of RNA-mediated immunotherapy based on the concept of molecular mimicry. I identified a mechanism in AML-bearing mice that led to immune cell-mediated rejection of tumor cells, establishing complete remission and vaccine-like immunity in a fraction of the animals.

1.1 AML

1.1.1 Epidemiology and etiology

AML is a disease predominantly found in elder patients with a peak incidence at an age beyond 80 years (Dores et al. 2012). In 2018, an estimated number of 10,670 patients succumbed to lethal complications of AML in the United States of America according to the National Institute of Health (NIH), making up 1,8% of all cancer related deaths in the USA. Despite some improvements in therapeutic and diagnostic strategies over the past years, AML remains a medical condition with a poor prognosis and a problematic relapse rate.

The disease originates from the bone marrow, where red and white blood cells mature from early progenitor cells. Adaptive immune cells derive from lymphatic stem cells whereas granulocytes amongst other cell types derive from myeloid stem cells. Genetic predisposition, hematologic diseases and environmental factors like exposure to radiation can increase the risk of acquiring mutations which may lead to malignant transformation of an immature myeloid precursor

cell (Link et al. 2007, Yoshimi et al. 2014), meaning the cell becomes independent of growth factors and acquires immortality while losing the ability to differentiate. This tumor cell can now clonally expand in the bone marrow and suppress physiological hematopoiesis, eventually leading to a lack of functional immune cells (Tenen et al. 1997), erythrocytes and thrombocytes in the peripheral blood. The lack of these cells explains the common immunodeficiency, anemia and bleeding disorders prevalent in AML patients. Malignant cells of the bone marrow can pass into the blood stream, leading to elevated numbers of white blood cells in the peripheral blood. This phenomenon is eponymous for the disease which translates from ancient Greek as "white (λευκός/*leukós*) blood (αἷμα/*haima*)".

1.1.2 Treatment of AML

In the past, three main strategies were established for the treatment of cancer: Surgical procedures, radiation and chemotherapy. In AML, the latter is of highest relevance. For a fraction of patients, intensive chemotherapy followed by stem cell transplantation (SCT) remains the only curative treatment option (Dohner et al. 2015). However, treatment-related morbidity and mortality as well as numerous contraindications for this approach, including high age, chronic or acute infectious disease and relapsed disease state after repeated SCT, make alternative treatment strategies urgently needed.

Recent developments gave rise to immunotherapeutic approaches, the basic concept of which is to utilize the patient's immune system to eradicate cancerous cells. While SCT is considered one of the earliest immunotherapies in history, novel approaches regarding AML include antibody-based therapy, CAR T cells, dendritic cell (DC) vaccination and checkpoint inhibition (Dohner et al. 2015, Lichtenegger et al. 2017). These treatments have only recently been implemented in clinical trials and their full potential for clinical use remains elusive at this point.

1.2 Innate immune receptors and adaptive immunity

The human organism is constantly exposed to potentially harmful pathogens such as microorganisms and viruses. The immune system of our body prevents us from falling victim to most of them by surveilling all potential sites of entry and neutralizing pathogens that breached outer barriers. Further, the immune system holds the ability to identify and kill cells that have undergone pathologic transformation, including cancer cells. Innate immunity as opposed to adaptive immunity forms the first line of defense, enabling rapid induction of immune defense mechanisms based on the recognition of non-self or foreign molecular patterns. The activation of the innate immune system is the prerequisite for the initiation of an antigen-specific adaptive immune response. To this end, innate immune cells take up and present foreign antigens to lymphocytes while fueling and shaping the adaptive immune response via the secretion of cytokines and chemokines. Thus, both branches of the immune system are linked and merge into one another in the course of an immune response (Janeway et al. 2001).

1.2.1 The innate immune system

The epithelial barrier of our skin, the complement system and phagocytic cells are just few examples of what the innate immune system is composed of. Innate immunity is largely based on the concept of pattern recognition, allowing it to discriminate between self and non-self antigens (Janeway 1989, Brubaker et al. 2015). Certain molecular patterns are shared amongst and indicative of foreign antigens, referred to as pathogen-associated molecular patterns (PAMPs) (Mogensen 2009). A wide range of pattern recognition receptors (PRRs) is responsible for the detection of PAMPs and the induction of an adequate immune response, which involves the activation of adaptive immune cells. Thus, PRRs create a link between innate and adaptive immunity. In this work, I focus on innate PRRs involved in the detection of nucleic acids.

1.2.1.1 RIG-I

Retinoic acid-inducible gene-I-like receptors (RLR) are a family of innate PRRs involved in anti-viral defense. The receptor family consists of retinoic-acid inducible gene I (RIG-I), melanoma differentiation-associated 5 (MDA5) and laboratory of genetics and physiology 2 (LGP2). These cytoplasmic receptors are ubiquitously expressed at different levels, even in tumor cells (Onoguchi et al. 2011), and sense viral RNA. RIG-I is of central interest to my work and is known to bind short double-stranded (ds) viral RNA (Schlee et al. 2009). While endogenous nuclear RNA gets modified with a five-prime (5') cap when leaving the nucleus, viral RNA often remains uncapped, leaving the 5' triphosphate (ppp) ending of the RNA exposed. The 5'-ppp pattern allows to discriminate between exogenous and endogenous RNA, making short RNAs with an uncapped 5'-ppp ending (ppp-RNA) the natural ligand of RIG-I (Hornung et al. 2006).

Upon binding to viral RNA, RIG-I triggers two different signaling cascades. On the one hand, RIG-I undergoes conformational change and exposes its caspase activation and recruitment domains (CARDs) to interact with the adaptor mitochondrial antiviral-signaling protein (MAVS) (Chow et al. 2018). MAVS, an outer membrane-bound mitochondrial adaptor protein, in turn assembles numerous downstream signaling proteins culminating in the activation of nuclear factor kappa-light-chain-enhancer of activated B cells (NF-κB) and interferon regulatory factor 3/7 (IRF3/IRF7), resulting in the release of type I and type III interferons (IFN) and proinflammatory cytokines (Kell et al. 2015, Hemann et al. 2017). The cytokine release induces an adaptive immune response targeted against infected cells, mainly mediated by cluster of differentiation (CD) 8$^+$ T cells and natural killer (NK) cells (Poeck et al. 2008).
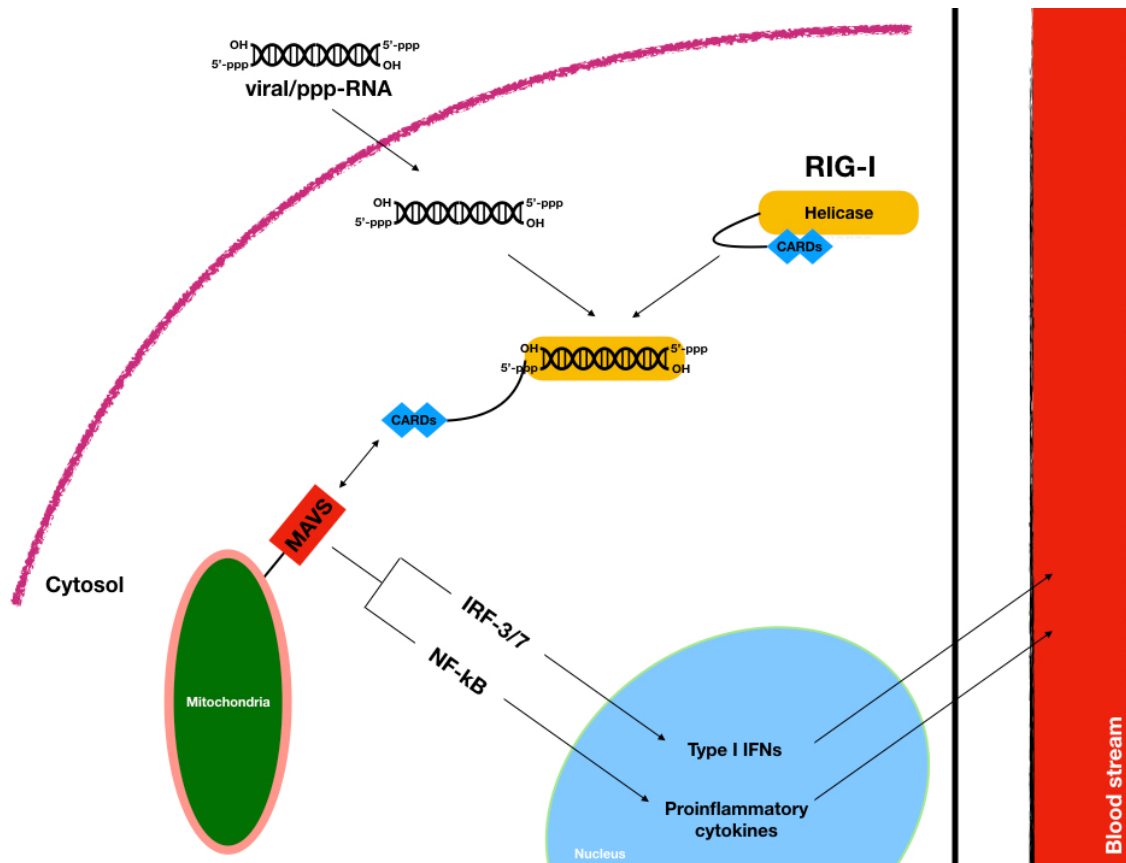
Illustration 1. RIG-I signaling. RIG-I senses cytoplasmic viral or synthetic ppp-RNA, which leads to a conformational change of the receptor and exposure of its active CARDs. These can now interact with MAVS, an outer mitochondrial membrane-bound adaptor protein. MAVS triggers further downstream signaling via NF-kB and IRF-3/7, inducing the transcription of type I IFNs and proinflammatory cytokines which eventually lead to systemic immune activation.

Apart from cytokine release, RIG-I activation has been described to induce an immunogenic form of cell death in infected cells (Besch et al. 2009). RIG-I induced apoptosis is IFN independent and relies on the proapoptotic protein NOXA, further involving caspase-9 and apoptotic protease-activating factor-1 (APAF-1) (Duewell et al. 2014). This mechanism can be considered as a means of confining virus spread by swift elimination of infected cells before neighboring cells are affected.

1.2.1.2 Toll-like receptors

Another family of PRRs play a central role in innate immunity: the toll-like receptors (TLRs). 10 different subtypes, labeled TLR1-10, are found in humans, predominantly expressed on antigen presenting cells (APCs) such as DCs and macrophages. A subset of TLRs is also present in non-immune cells (Kawasaki et al. 2014). TLRs sense various kinds of PAMPs found in viruses and microorganisms such as bacteria, protozoa and fungi (Blasius et al. 2010). In the context of my work, the intracellular TLR7 is of particular interest since it has the ability to sense microbial- and virus-derived RNA (Blasius et al. 2010), and thus ppp-RNA, too (Hornung et al. 2005). Once TLRs bind to their respective antigen, they trigger TLR subtype-specific signaling cascades that result in the release of proinflammatory cytokines, initiating an adaptive immune response (Janeway et al. 2002) similarly to RIG-I.

1.2.2 The adaptive immune system

In contrast to PAMP-based innate immune surveillance, adaptive immunity operates in an antigen-specific way. Adaptive immunity is mediated by B and T lymphocytes or B and T cells, which express highly specific antigen receptors on their surface. The broad range of antigens covered is explained by somatic recombination, a process in which genes coding for these surface receptors are recombined, resulting in a large variety of the translated receptors (Livak et al. 2000). These B and T cell receptors (BCR, TCR) recognize specific foreign antigens. While B cells are able to recognize antigens directly, T cells are restricted to antigens presented on the surface of APCs in the context of major histocompatibility complex (MHC) molecules (Janeway et al. 2001). Binding of the antigen together with essential co-stimuli results in the activation of the respective lymphocyte, followed by clonal expansion of the same (Obst 2015). This enables a systemic, antigen-specific immune response. Of note, the adaptive immune system establishes an immunological memory after first antigen

contact, accelerating future immune responses after re-exposure (Pascutti et al. 2019).

While B cells secrete neutralizing and opsonizing antibodies upon antigen contact, T cells and their function can be classified further: Cytotoxic T cells characteristically express CD8 on their surface and are thus commonly referred to as CD8^{+} T cells. They have the ability to kill infected or cancerous cells and microorganisms. T helper cells or CD4^{+} T cells play a supportive role via their ability to release cytokines responsible for the activation of CD8^{+} T, B and other immune cells.

1.2.3 Interferons

Interferons (IFNs) are a group of proteins involved in the mediation of predominantly anti-viral, but also anti-microbial (Stanifer et al. 2019) and anti-tumor defense (Takaoka et al. 2003, Studeny et al. 2004). PRRs such as RIG-I and TLRs are main triggers of its release. In humans, the following interferons are of highest relevance: IFN-alpha (IFNα - a group of 13 highly related proteins in humans and 14 in mice (van Pesch et al. 2004)), IFN-beta (IFNβ), IFN-gamma (IFNγ) and IFN-lambda (IFNλ). IFNα and IFNβ belong to the family of type I IFNs, whereas IFNγ is considered type II IFN and IFNλ type III IFN (Hoffmann et al. 2015).

Type I IFNs are released by virus-infected cells. In proximity to the source of infection, they induce the expression of anti-viral proteins via the IFNα/β receptor 1 (IFNAR1) and 2 (IFNAR2), which are ubiquitously expressed on nucleated cells (Hoffmann et al. 2015). Apart from proteins directly inhibiting viral replication, the expression of proteins required for the processing and presentation of antigens on major histocompatibility complex class I (MHC-I) and class II (MHC-II) molecules is also stimulated by IFN, resulting in increased antigen-presentation on the cell surface. This facilitates antigen-recognition by immune cells and the initiation of an adaptive immune response. The augmented immune surveillance leads to further increased levels of INFs and other

proinflammatory cytokines in a positive-feedback manner, as more foreign antigens may be detected (Ma et al. 2015).

Type II IFN is released by T and NK cells as well as other immune cells upon activation. The effects of type II IFN on surrounding cells are similar to the effects of type I IFNs. Type III IFNs show mainly anti-viral properties and do also induce the expression of interferon-stimulated genes. In contrast to type I IFNs though, their action is mainly restricted to mucosal surfaces of epithelial barriers as found in the gastrointestinal and respiratory tract (Hemann et al. 2017). Thus, their contribution to systemic anti-viral defense is subordinate (Major et al. 2020).

Lastly, type I, II and III IFNs may display a pro-apoptotic effect on and reduce the proliferation of virally infected and cancer cells by boosting the activity of p53, a tumor suppressor protein also known to inhibit angiogenesis (Takaoka et al. 2003, Major et al. 2020).

1.3 Immunotherapy of cancer

The immunotherapy of cancer is an emerging field in modern medicine. It is founded on the perception that the human immune system has means at its disposal to identify and combat cancer cells. These means, however, are circumvented by so called immune escape mechanisms of the tumors. Numerous immune escape mechanisms have been identified of which many serve as points of action for immunotherapeutic interventions. The most prominent example is the identification of immune checkpoints and their therapeutic antagonization.

1.3.1 Immune checkpoint inhibition

Immune checkpoints are molecular structures promoting or inhibiting the immune system's activity. Cytotoxic T-lymphocyte-associated protein 4 (CTLA-4) and the programmed cell death protein 1 (PD-1) / programmed death-ligand 1 (PD-L1) axis are the most prominent examples since blocking antibodies against them are

already approved for certain tumor entities or currently subject of clinical trials. Of these two examples, the PD-1/PD-L1 axis is of particular interest to my studies.

PD-1 is expressed on the surface of immune cells and was initially discovered as an inhibitory immune regulator in the context of autoimmune disease and apoptosis studies (Ishida et al. 1992, Bardhan et al. 2016) with great importance for self-tolerance. Upon binding to its natural ligand PD-L1, it inhibits T cell proliferation and restricts IFNγ secretion. PD-L1 shows broad, IFN-dependent expression and is often found highly expressed on the surface of tumor cells (Bardhan et al. 2016). Immune responses against tumor cells go along with elevated levels of IFN and may thus upregulate PD-L1 expression on cancer cells, which in turn can now easier interact with PD-1 on immune cells and limit the immune response.

The inhibitory PD-1/PD-L1 axis can be disrupted with blocking antibodies directed against either one of the molecules. In recent years, these so-called checkpoint inhibitors have been tested in numerous tumor entities with great success (Bald et al. 2014, Gubin et al. 2014, Tumeh et al. 2014, Robert et al. 2015, Ascierto et al. 2018), disinhibiting the PD-1/PD-L1 axis and resulting in increased cytotoxic activity of T cells. In contrast, checkpoint inhibition was less successful as a monotherapy for AML in both clinical settings (Lichtenegger et al. 2017) and the preclinical AML mouse model C1498, which is used in this thesis (Zhang et al. 2009).

1.3.2 RIG-I in tumor therapy[1]

RLR ligands have shown to be a promising strategy in the preclinical treatment of numerous solid malignancies including melanoma (Poeck et al. 2008) and pancreatic cancer (Ellermeier et al. 2013), just recently qualifying for a combined phase I/II study in patients with advanced solid tumors (NCT03065023). The cytokine release triggered by RIG-I combined with direct sensing of viral RNA by

---

[1] With some modifications as described in Ruzicka, Koenig et al. 2020

immune cells enhances recognition of foreign antigens by upregulating the expression of MHC and co-stimulatory molecules, and by activating immune cells. By applying an exogenous short ppp-RNA, a viral infection can be mimicked, allowing a direction of the immune response towards otherwise altered or potentially harmful targets, such as tumor cells. Furthermore, ppp-RNA has been shown to induce an immunogenic form of cell death which interestingly, tumor cells are more susceptible to than nonmalignant cells (Besch et al. 2009, Duewell et al. 2014). While RIG-I targeted immunotherapy has shown beneficial effects on survival in different solid tumor models, its efficacy in non-solid tumor models has not been studied so far.

1.4 Objectives

The primary objective of this study was to evaluate the potential of ppp-RNA therapy in a non-solid malignancy. Due to the prominent role of systemic IFN and cytokine release involved in RIG-I-targeted treatment as well as the possible systemic, intravenous (i.v.) application route of ppp-RNA, hypothetically, hematologic tumors should be particularly responsive to this treatment. AML was chosen as an example of such a hematologic malignancy.

Previously, our group validated RIG-I *in vitro* as a potential target for the treatment of AML using human AML cell lines. Interferon release as well as apoptosis of transfected cells was observed, raising the question as to whether these findings could be translated *in vivo*. The C1498 AML cell line is the only available syngeneic murine AML cell line and thus the choice for my *in vivo* studies. In this thesis, I raised and investigated the following questions:

- Does ppp-RNA treatment affect the tumor burden and survival of mice bearing systemic C1498 AML?

- Which immune cells mediate ppp-RNA-induced tumor rejection?

- To what extent does the treatment with ppp-RNA rely on RIG-I signaling in host cells?

- What is the role of IFN signaling in the host?

- Does successful treatment of AML with ppp-RNA induce an adaptive immune response including the formation of an immunological memory?

- ppp-RNA treatment induces the upregulation of PD-L1 on tumor cells via IFN. Does the addition of PD-1 checkpoint blockade therapy result in enhanced overall survival?

- Can effects of ppp-RNA therapy in a murine model of AML be translated into a humanized mouse model of AML?

2. Materials and Methods

2.1 Materials

2.1.1 Laboratory hardware

Product name	Manufacturer	Production site
ÄKTAmicro (high pressure liquid chromatography)	GE Healthcare Life Sciences	Massachusetts, USA
Centrifuge 5418r	Eppendorf	Hamburg, Germany
Centrifuge Rotina 420R	Hettich GmbH	Tuttlingen, Germany
CO2 – Incubator (BD6220)	Heraeus, ThermoFischerScientific	Massachusetts, USA
DNAPac 200 column	Thermo Fisher Scientific	Germering, Germany
FACSCanto II	BD Biosciencess	New Jersey, USA
FACSCalibur Flow Cytometry System	BD Biosciencess	New Jersey, USA
Refridgerator 4°C	Bosch	Gerlingen-Schillerhöhe, Germany
Freezer -20°C	Bosch	Gerlingen-Schillerhöhe, Germany
Hemocytometer - Neubauer	MTG GmbH	Bruckberg, Germany
HERAfreezeTM HFU T Series	Heraeus, ThermoFischerScientific	Massachusetts, USA
Hood 2-453-JAND	Köttermann GmbH & Co KG	Hänsingen, Germany
Innova44 Thermoshaker	New Brunswick Scientific, Eppendorf	Hamburg, Germany
Laminair HB 2472 S cell culture flow	Heraeus, ThermoFischerScientific	Massachusetts, USA
Light microscope Axiovert 40C	Zeiss	New York, USA
LS Columns	Miltenyi Biotec	Bergisch Gladbach, Deutschland
MACS SmartStrainers (30, 70 and 100 µm)	Miltenyi Biotec	Bergisch Gladbach, Deutschland
LSRFortessa	BD Biosciencess	New Jersey, USA
Magnetspinning RH BASIC 2	IKA	Staufen, Germany

MicroWell plates ELISA, Costar Assay Plate, 96 well	Corning	Corning (New York), USA
Mini Trans-Blot® Cell	Bio-Rad Laboratories	Munich, Germany
MiniMACS, QuadroMACS Separator	Miltenyi Biotec	Bergisch Gladbach, Deutschland
Mithras lb 940	Berthold Technologies	Bad Wildbad, Germany
Multifuge 3L-R, X3 and 4KR	Heraeus, ThermoFischerScientific	Massachusetts, USA
Nanodrop 2000c Spectrophotometer	ThermoFischerScientific	Massachusetts, USA
Neubauer counting chamber	Optik Labor Frischknecht	Balgach, Germany
pH-Meter	WTW	Weilheim, Deutschland
Pipetus	Hirschmann	Eberstadt, Germany
PowerPacTM Universal Power Supply	Bio-Rad Laboratories	Munich, Germany
Research plus pipet sets	Eppendorf	Hamburg, Germany
Rollershaker CAT RM 5	Ingenieurbüro CAT, M. Zipperer GmbH	Germany
Sprout minicentrifuge	Biozym	Hessisch Oldendorf, Germany
T3 Thermocycler	Biometra	Göttingen, Germany
Table vortexer RS VA 10	Phoenix	Garbsen, Germany
Thermomixer comfort	Eppendorf	Hamburg, Germany
Vortex	Janke & Kunkel	Staufen, Germany
Welch vacuum pump	Promega	Wisconsin, USA

2.1.2 Reagents, chemicals, buffers and kits

Product name	Manufacturer	Production site
Albumin Fraction V (BSA)	Sigma-Aldrich	Steinheim, Germany
BD Pharm Lyse Lysing Buffer (10x)	BD Biosciences	New Jersey, USA
Biocoll Separating Solution	Merck	Darmstadt, Germany

CD8a+ T Cell Isolation Kit mouse	Miltenyi Biotec	Bergisch Gladbach, Germany
Colagenase D	Sigma-Aldrich	Steinheim, Germany
Count Bright, counting beads	LifeTechnologies	California, USA
DCTM Protein Assay	Bio-Rad Laboratories	Munich, Germany
Dimethylsulfoxid (DMSO)	Sigma-Aldrich	Steinheim, Germany
DNase I	Roche	Mannheim, Germany
Dulbecco's phosphate buffered saline (PBS)	PAA Laboratories	Pasching, Austria
Ethanol 100%	Carl Roth GmbH	Karlsruhe, Germany
FACSFlow, FACSSafe	BD Biosciences	New Jersey, USA
Heparin-sodium 2.500 IE / 5ml	Braun AG	Melsungen, Germany
Isofluoran	CP PHARMA	Burgdorf, Germany
Mouse CXCL10/IP-10/CRG-2 DuoSet ELISA	R&D Systems	Minnesota, USA
HiScribe™ T7 Quick High Yield RNA Synthesis Kit	New England BioLabs Inc.	Massachusetts, USA
Human CXCL10/IP-10 DuoSet ELISA	R&D Systems	Minnesota, USA
Powdered milk, blotting grade	Carl Roth GmbH	Karlsruhe, Germany
Sodium chloride	Sigma-Aldrich	Steinheim, Germany
Sulphuric Acid	Apotheke Innenstadt	LMU Munich, Germany
Tissue freezing medium	Leica biosystems	Nussloch, Germany
Total RNA Clean-Up and Concentration Kit	Norgen Biotek	Ontario, Canada
Trypan-Blue	Sigma-Aldrich	Steinheim, Germany
Tween 20	Carl Roth GmbH	Karlsruhe, Germany

2.1.3 Cell culture reagents, cytokines, beads and media

Product name	Manufacturer	Production site
Anti-mouse CD3ε	BD Pharmingen	New Jersey, USA
Anti-mouse CD28	BD Pharmingen	New Jersey, USA
Recombinant human IL-2	Chiron (Novartis)	Basel, Switzerland
Recombinant human IL-15	Preprotech	Hamburg, Germany
Dynabeads Mouse T-Activator CD3/CD28	Invitrogen (ThermoFischerScientific)	Massachusetts, USA
Dulbecco's Modified Eagle's Medium (DMEM)	Lonza	Verviers, Belgium
HEPES-Buffer 1M	Sigma-Aldrich	Steinheim, Germany
High Glucose Fetal Bovine Serum (FBS)	Gibco Products	New York, USA
L-Glutamin 200mM	PAA Laboratories	Pasching, Austria
MEM Non-essential amino acids (NEAA, 100x)	Gibco Products	New York, USA
Opti-MEM® Medium	Gibco Products	New York, USA
Sodium pyruvate	Sigma-Aldrich	Steinheim, Germany
Penicillin/Streptomycin (100x)	PAA Laboratories	Pasching, Austria
Roswell Park Memory Institute (RPMI)	Lonza	Verviers, Belgium
ß-Mercaptoethanol	Sigma-Aldrich	Steinheim, Germany
Trypsin (10x)	PAA Laboratories	Pasching, Austria
Plastic materials (flasks, well plates and others) for cell culture	BD Falcon Corning Greiner Bio-One Sartorius	Franklin Lakes NJ, USA Corning New York, USA Kremsmünster, Germany Göttingen, Germany

2.1.4 *In vivo* antibodies

Target	Clone	Catalog number	Manufacturer	Production site
anti-mouse CD4	GK1.5	BE0003-1	Bio X Cell	New Hampshire, USA
anti-mouse CD8a	YTS 169.4	BP0117	Bio X Cell	New Hampshire, USA
anti-mouse CD19	1D3	BE0150	Bio X Cell	New Hampshire, USA
anti-mouse NK1.1	PK136	BE0036	Bio X Cell	New Hampshire, USA
rat IgG2b	LTF-2	BE0090	Bio X Cell	New Hampshire, USA
mouse IgG2a	C1.18.4	BP0085	Bio X Cell	New Hampshire, USA
rat IgG2a	2A3	BP0089	Bio X Cell	New Hampshire, USA
anti-mouse PD-1	RMP1-14	BP0146	Bio X Cell	New Hampshire, USA

2.1.5 Antibodies for flow cytometry

Antibody	Fluorochrome	Clone	Catalog number	Manufacturer	Production site
anti-human CD3	APC	OKT3	317318	BioLegend	California, USA
anti-human CD3	Pacific Blue	UCHT1	300431	BioLegend	California, USA
anti-human CD3	FITC	UCHT1	300406	BioLegend	California, USA
anti-human CD8	APC	REA734	130110679	Miltenyi Biotec	Bergisch Gladbach, Germany
anti-human CD20	Pacific Blue	2H7	302328	BioLegend	California, USA
anti-human CD33	APC	P67.6	366605	BioLegend	California, USA
anti-human CD45	FITC	2D1	368508	BioLegend	California, USA
anti-human pan-CD45	PE	2D1	368510	BioLegend	California, USA

anti-human PD-L1	PE/Cy7	29E.2A3	329717	BioLegend	California, USA
anti-mouse CD45	Pacific Blue	30-F11	103126	BioLegend	California, USA
anti-mouse CD45	PerCP	30-F11	103130	BioLegend	California, USA
anti-mouse CD3ε	APC	145-2C11	100312	BioLegend	California, USA
anti-mouse CD4	PE	GK1.5	553730	BD Biosciences	New Jersey, USA
anti-mouse CD4	PE/Cy7	RM4-5	100528	BioLegend	California, USA
anti-mouse CD8a	APC	53-6.7	553035	BD Biosciences	New Jersey, USA
anti-mouse CD8	PE	53-6.7	100708	BioLegend	California, USA
anti-mouse NK1.1	PerCP	PK136	108726	BioLegend	California, USA
anti-mouse PD-L1	PE/Cy7	10F.9G2	124314	BioLegend	California, USA
anti-mouse CD19	PE	6D5	115508	BioLegend	California, USA
anti-mouse CD45	Alexa-Fluor 700	30-F11	103128	BioLegend	California, USA
mouse IgG1, κ	APC	MOPC-21	400120	BioLegend	California, USA
mouse IgG1, κ	FITC	MOPC-21	555748	BD Biosciences	New Jersey, USA
mouse IgG1, κ	Pacific Blue	MOPC-21	400151	BioLegend	California, USA
mouse IgG1, κ	PE	MOPC-21	400112	Biolegend	California, USA
mouse IgG2a, κ	APC	MOPC-173	400220	BioLegend	California, USA
mouse IgG2a, κ	PerCP	MOPC-173	400256	BioLegend	California, USA
rat IgG2a, κ	PE	RTK2758	400507	BioLegend	California, USA
rat IgG2a, κ	PE/Cy7	RTK2758	400522	BioLegend	California, USA
rat IgG2b, κ	PE/Cy7	RTK4530	400618	BioLegend	California, USA

rat IgG2b, κ	PerCP	RTK4530	400629	BioLegend	California, USA
mouse IgG2b, κ	Pacific Blue	MPC-11	400331	BioLegend	California, USA
eBioscience™ Fixable Viability Dye	eFluor™ 780		65-0865-18	Thermo Fisher Scientific	Germering, Germany
TO-PRO™-3 Iodide (642/661)			T3605	Thermo Fisher Scientific	Germering, Germany

2.1.6 Cell culture media

DMEM supplemented

Medium / supplement	Volume / concentration
DMEM	500 ml
FBS	10 %
L-glutamine	1.5 mM
Penicillin	100 IU/ml
Streptomycin	100 µg/ml

T cell medium

Medium / supplement	Volume / concentration
RPMI	500 ml
FBS	10 %
L-glutamine	1.5 mM
Penicillin	100 IU/ml
Streptomycin	100 µg/ml
HEPES-Buffer	0.5 mM
Sodium pyruvate	1 mM

PDX AML cell medium

Composure not disclosed. Kindly provided by I. Jeremias (Research Unit Apoptosis in Hematopoietic Stem Cells, Helmholtz Zentrum München, German Research Center for Environmental Health (HMGU), Munich, Germany).

2.2 Cellular methods

2.2.1 Cells[2]

Murine C1498 AML cells were purchased from ATCC (TIB-49TM) and retrovirally transduced with an enhanced green fluorescent protein (eGFP) using a pMX-eGFP plasmid and the PlatE viral producer cell line by E. M. Heuer (Abt. für Klinische Pharmakologie, Medizinische Klinik IV, LMU Munich). Positive cells were sorted via flow cytometry and pooled for further use. The human 1205Lu melanoma cell line was kindly provided by R. Besch (Klinikum der Universität München, Department of Dermatology, Munich, Germany). Patient-derived xenograft (PDX) AML cells were produced by serial re-transplantation of primary patient leukemic cells in NOD-*scid* IL2Rγ^{null} (NSG) mice as described previously by Vick et al. (Vick et al. 2015). I utilized the mCherry-positive PDX AML 491 cell line which was derived from a 53-year-old female patient at a relapsed disease stage classified as adverse according to the European LeukemiaNet classification system. All cell lines were regularly checked for mycoplasma contamination.

2.2.2 Cell culture conditions

Cells were cultivated at a temperature of 37°C, 95% humidity and a CO_2 concentration of 5%. Tumor cell lines were cultivated in supplemented DMEM, PDX AML cells were cultivated in medium provided by I. Jeremias. The density

---

[2] With some modifications as described in Ruzicka, Koenig et al. 2020 (Supplementary materials and methods)

of C1498 AML cells was adjusted daily to 1×10^5 cells/ml, the density of other cells according to the specific needs. All procedures were carried out under sterile conditions under a laminar flow hood.

2.2.3 Counting of cells

Adherent cells were washed with Phosphate buffered saline (PBS) and loosened from the flask surface by incubation in trypsin at 37°C. The reaction was stopped with cell culture medium after 5-15 minutes. Adherent and suspension cells were stained by addition of 0.25% trypan blue in PBS, a dye staining dead cells. The viability and density of the cells was determined under a microscope using a "Neubauer" cell counter composed of four chambers. Taking the dilution of the cells by the dye into consideration, the cell number per ml was determined by multiplying the number of viable cells counted in one chamber by the dilution factor and 10^4.

2.2.4 Freezing and thawing of cells

Cells were counted, pelleted by centrifugation and resuspended in FBS containing 10% DMSO. At a density of 4×10^6 to 7×10^6 cells per ml, the cell suspension was distributed into cryo-tubes and frozen at -80°C. For mid- and long-term storage, the cells were transferred to liquid nitrogen 48 hours later.

Cells were thawed by quick resuspension in 37°C warm cell medium. Viability and cell number were determined before the cells were washed and resuspended in an appropriate volume of suitable medium for further cultivation.

2.2.5 Human peripheral blood mononuclear cells

Venous blood was withdrawn by means of a winged infusion set and a 50 ml syringe, using 200 IE Heparin as anticoagulant. The blood was then diluted with 0.9% NaCl solution at a ratio of 1.25 : 1 (blood : NaCl). 15 ml of Biocoll Separating Solution were pipetted into a 50 ml polypropylene tube and diluted blood was slowly added on top, forming two liquid phases. The tubes were then centrifuged at 1000 g for 20 minutes at room temperature. The break of the centrifuge was disabled to assure an accurate phase distribution along the density gradient. The visible layer of peripheral blood mononuclear cells (PBMCs) was harvested with a pipetus and washed with sterile PBS thrice. The cells were then frozen or re-suspended in PBS for immediate further use.

2.2.6 *In vitro* transfection

For the *in vitro* lipofection of 1205Lu melanoma cells, RNA was complexed using Lipofectamine^{TM} RNAiMAX Transfection Reagent (ThermoFisher). 80 nM of RNA and 0.5 µl of the transfection reagent were each diluted in 25 µl of Opti-MEM$^{®}$ Medium. Subsequently, the diluted RNA was added to the diluted transfection reagent and placed into a 96-well culture dish at 10 µl per well to form complexes. After an incubation period of 5 minutes, 12.5×10^3 1205Lu melanoma cells in a volume of 100 µl Opti-MEM$^{®}$ Medium were added in a manner of reverse transfection. The mixture was incubated under the conditions described in 2.2.2 for 12-24 hours before the samples were further analyzed.

2.2.7 Magnetic-activated cell sorting

In my studies, I sought to negatively select CD8$^+$ T cells from splenocyte single cell suspensions using the CD8a$^+$ T Cell Isolation Kit mouse according to the manufacturer's protocol for manual magnetic labeling and extraction. First, the cell suspension was treated with a cocktail of biotin labeled antibodies which

specifically exclude surface structures of CD8+ T cells. In a second step, magnetic Anti-Biotin MicroBeads were added, binding to the biotin labeled antibodies. The cell suspension was passed through a LS Column embedded in the magnetic field of a QuadroMACS-Separator. While magnetically labeled cells were held back and remained in the column, the flow-through contained the desired CD8+ T cells. To validate the purity of the product, I stained a portion of the obtained cells with anti-CD3 and anti-CD8a fluorescent antibodies and analyzed them by flow cytometry, revealing a viable, double positive T cell fraction of > 98% in the flow through.

2.3 Immunological methods

2.3.1 Enzyme-linked immunosorbent assay

Chemokine levels were measured via enzyme-linked immunosorbent assay (ELISA). I used the Mouse CXCL10/IP-10/CRG-2 DuoSet ELISA (R&D Systems) to detect serum chemokine levels of murine CXCL-10 4 hours after ppp-RNA treatment of mice. Levels of human CXCL10 in tumor cell supernatants were analyzed 24 hours after transfection using the human CXCL10/IP-10 DuoSet ELISA. ELISA was performed as described in the manufacturers protocol. The CXCL10 concentration of the respective samples was calculated using Microsoft Excel version 14.0.0.

2.3.2 Flow cytometry

Flow cytometry or fluorescence-activated cell sorting (FACS) allows to investigate the expression of extra- and intracellular markers of single cells using fluorescent antibodies. Cell suspensions can be analyzed to determine their composition with regard to cell phenotypes or to investigate the expression level of markers on specific cells.

The flow cytometry data in this thesis were raised with three different devices:

Device	Manufacturer	Lasers
BD FACSCalibur	BD Biosciences	488 nm, 635 nm
BD FACSCanto II	BD Biosciences	405 nm, 488 nm, 633 nm
BD LSRFortessa	BD Biosciences	405 nm, 488 nm, 561 nm, 633 nm

Table 1: Flow cytometers. Names, manufacturers and available lasers of flow cytometers used to generate the data presented in this thesis are depicted.

1×10^6 single cells were re-suspended in 100 µl PBS and stained with fluorescent antibodies at a concentration of 5 µl/ml. After an incubation time of 30 minutes at 4°C in the absence of light, remaining antibody was washed off with PBS. The cells were again re-suspended in 100 µl PBS and analyzed with the flow cytometer. FACS data were then processed using FlowJo software version 8.

2.4 ppp-RNA synthesis

In vitro transcription (IVT) is a cost-efficient method to produce RNA for scientific use. For my studies, I chose the T7 DNA-dependent RNA polymerase to form RNA from a double-stranded DNA-template containing the T7 promoter sequence. Products of the reaction contain a 5'-triphosphate moiety. The IVT product was purified, and its functionality was assessed before further use as described below.

2.4.1 *In vitro* transcription and purification of ppp-RNA[3]

The following single-stranded DNA oligonucleotides were purchased from Metabion (Planegg, Germany), annealed in a thermo cycler (85°C for 5 minutes

---

[3] With some modifications as described in Ruzicka, Koenig et al. 2020 (Supplementary materials and methods)

followed by gradual cooling down to 4°C at 0.1°C/s) to form a double-stranded DNA-template and subsequently used for the IVT reaction.

Name	Sequence (5' -> 3')
CO4 sense DNA template	*TAATACGACTCACTATA***GCG**CTATCCAGCTTACGTAGAGCT CTACGTAAGCTGGATAGCGC
CO4 anti-sense DNA template	GCGCTATCCAGCTTACGTAGAGCTCTACGTAAGCTGGATA G**CGC***TATAGTGAGTCGTA*

Table 2: Sequences of DNA-templates used for IVT. High pressure liquid chromatography (HPLC)-purified single-stranded complementary DNA-templates for IVT of ppp-RNA were purchased from Metabion (Planegg, Germany). The T7 Promoter is highlighted in italic font while bold letters mark the starting point of the transcription.

The template was transcribed using the HiScribe™ T7 Quick High Yield RNA Synthesis Kit according to the manufacturer's protocol. The reaction was started using 10 µl of a nucleoside triphosphate (NTP) containing buffer mix, 2 µM of DNA-template, 2 µl of T7 RNA Polymerase Mix and 15 µl of nuclease-free water. An incubation period of 16 hours at 37°C followed. The DNA template was digested by addition of DNase I to the mix and incubation at 37°C for 30 minutes. Contaminants like enzymes and NTPs were removed from the IVT product by means of the Total RNA Clean-Up and Concentration Kit (Norgen Biotek), following the manufacturer's protocol. ppp-RNA concentration was measured with a spectrophotometer. Purity of the product was determined by HPLC using a DNAPac 200 column. Industrially synthesized ppp-RNA served as a control for peak analyses.

Table 3 shows the ppp-RNA sequence as well as the sequence of OH-RNA, which was used as a control. OH-RNA has the identical sequence as ppp-RNA but lacks both the hairpin loop structure and the 5'-ppp ending.

Name	Sequence (5' -> 3')
ppp-siCO4 hp (ppp-RNA)	ppp-GCGCUAUCCAGCUUACGUA *GAGCUC* UACGUAAGCU GGAUAGCGC
OH-siCO4 ds (OH-RNA)	OH-GCGCUAUCCAGCUUACGUA

Table 3: Sequences of RNA used for *in vitro* and *in vivo* studies. ppp-RNA was produced by *in vitro* transcription of a DNA-template. The loop forming base sequence of the hairpin (hp) structure is highlighted in italic font. Double-stranded (ds) OH-RNA was purchased from Metabion (Planegg, Germany).

As an additional quality control step, 1205Lu melanoma cells were transfected with 80 nM of *in vitro* transcribed ppp-RNA as described in 2.2.6. OH-RNA served as a control. After an incubation period of 24 hours, supernatants were harvested and levels of human CXCL10 were measured by ELISA to assess the functionality of the ppp-RNA.

2.5 Mouse studies

2.5.1 Mice[4]

In vivo studies were approved by the local regulatory agency (Regierung von Oberbayern, Munich, Germany). C57BL/6 mice were purchased from Janvier Labs, France. Mitochondrial antiviral-signaling protein knockout (*Mavs*^{-/-}) mice and interferon type I receptor knockout (*Ifnar1*^{-/-}) mice were kindly provided by U. Kalinke (TWINCORE Zentrum für Experimentelle und Klinische Infektions-forschung, Hannover, Germany). NOD-*scid* IL2Rγ[null] (NSG) mice were purchased from Charles River Laboratories. All animal experiments were carried out in the Zentrale Versuchstierhaltung Innenstadt of the Ludwig-Maximilians-Universität Munich.

---

[4] With some modifications as described in Ruzicka, Koenig et al. 2020 (Supplementary materials and methods)

2.5.2 AML inoculation[5]

C1498 AML cells were washed three times with PBS and viability as well as total cell number were determined as described in 2.2.3. The cell number was adjusted to 10^7 cells per ml PBS for the injection. At the age of 6 to 8 weeks, tumor inoculation of the mice was carried out by injecting $1x10^6$ C1498/GFP AML cells into the tail vein, defining day 0 of the experiment.

PDX AML cells were thawed, washed with PBS twice and the cell number was adjusted to $4.5x10^6$ cells per ml PBS. NSG mice were inoculated with $4.5x10^5$ cells i.v. on day 0 at the age of 5 weeks.

All mice were monitored daily and sacrificed at signs of affliction such as ascites, apathy, hunching, development of visible tumors and/or weight loss exceeding 15%. The signs were organized in a scoring system used to determine whether the sacrifice of an animal was due. In this work, the expression of mice dying reflects the sacrifice of animals when the respective criteria were met.

2.5.3 Complexation of RNA for *in vivo* treatment

For *in vivo* experiments, RNA was complexed with in vivo-jetPEI (Polyplus-transfection® SA), a cationic polymer-based transfection reagent. The non-viral vector is designed for systemic delivery of nucleic acids in animal models and has proven low cytotoxicity and limited immunogenicity according to the manufacturer's disclosures. RNA and in vivo-jetPEI were separately diluted into $^1/_2$ of the injection volume using sterile glucose solution (final glucose concentration: 5%) and water. Per 1 µg nucleic acid I used 0.12 µl of in vivo-jetPEI, corresponding to a N/P ratio of 6. The diluted in vivo-jetPEI mixture was added to the diluted RNA, vortexed gently and incubated for 15 minutes at room temperature to form complexes prior to further use.

---

[5] With some modifications as described in Ruzicka, Koenig et al. 2020 (Supplementary materials and methods)

2.5.4 *In vivo* treatment of AML[6]

ppp-RNA treatment (referring to ppp-RNA complexed with in vivo-jetPEI) was given via tail vein injection at a dose of 50 µg on days 3, 7, 10 and 14 (Figure 2A) if not stated differently. Murine interferon alpha (Miltenyi Biotec) was diluted in sterile PBS and administered via intraperitoneal (i.p.) injection on days 3, 7, 10 and 14 at a dose of $5x10^4$ IU. Anti-PD-1 antibody (αPD-1; clone: RMP1-14) or the corresponding isotype control rat IgG2a (clone: 2A3) were diluted in sterile PBS and given i.p. on days 6, 9 and 13 at a dose of 100 µg. PDX AML-bearing NSG mice were treated with 50 µg of ppp-RNA via tail vein injection on days 53, 56 and 59.

2.5.5 Immune cell depletion[6]

Depleting antibodies against CD4 (clone: GK1.5), CD8a (YTS 169.4), CD19 (1D3) and NK1.1 (PK136) were diluted in sterile PBS and injected i.p. at a dose of 250 µg on days 2, 6, 9 and 13. Rat IgG2b (LTF-2) served as an isotype control for anti-CD4 and CD8 antibodies, mouse IgG2a (C1.18.4) for the anti-NK1.1 antibody and rat IgG2a (2A3) for the anti-CD19 antibody, respectively. Immune cell depletion was validated via flow cytometry 24 hours after antibody injection.

2.5.6 Blood withdrawal and red blood cell lysis

Mice were anesthetized with 4% isoflurane in oxygen using an isoflurane vaporizer connected to a polymethylmethacrylat (PMMA) chamber. Blood was withdrawn retrobulbary with a heparinized glass cannula and stored at room temperature. After centrifugation, serum was removed and set aside for chemokine measurement. Red blood cells were lysed by applying 3 ml of BD Lysing Buffer twice for 5 minutes at room temperature. The reaction was stopped

---

[6] With some modifications as described in Ruzicka, Koenig et al. 2020 (Supplementary materials and methods)

with a 10-fold excess of PBS. White blood cells were resuspended in PBS or medium depending on the further progress.

2.5.7 *Ex vivo* analyses of solid organs

Mice were anesthetized with 4% isoflurane in oxygen and sacrificed by cervical dislocation. Solid organs (lungs, liver, spleen, ovaries, femurs, tibiae) were removed with surgical instruments. Epiphyses of bones were cut off, exposing the medullary cavity which was then flushed with PBS to obtain bone marrow samples. The remaining organs were incised with a scalpel multiple times before being incubated for 30 minutes at 37°C in 1 ml of a solution composed of 0.05 mg/ml DNAse and 1 mg/ml collagenase. The digested organs were passed through cell strainers and re-suspended in PBS. The resulting single cell suspensions, including bone marrow samples, were treated with erythrocyte lysing buffer (BD Lysing Buffer) as described in 2.5.6 and finally re-suspended in PBS for cell counting and further use.

2.5.8 Murine T cell transfer[7]

Spleens from C57BL/6 mice were extracted under a laminar flow hood and processed through 40 µm cell strainers. The resulting single cell suspension was treated with BD Lysing Buffer as described above. The obtained splenocytes were washed, resuspended in T cell medium and plated in a 6-well cell culture dish at a number of 2×10^6 cells/ml and 3 ml/well. For 24 hours, the cells were treated with 10 U/ml recombinant human IL-2, 1 µg/ml anti-mouse CD3e and 0.1 µg/ml anti-mouse CD28 antibodies. Next, the medium was changed and the cell number readjusted to 1×10^6 cells/ml. For 48 hours, the cells were expanded by the addition of 0.5 µg/ml IL-15. After expansion, CD8+ T cells were purified by negative selection MACS. Purity (> 98%) was validated via flow cytometry,

---

[7] With some modifications as described in Ruzicka, Koenig et al. 2020 (Supplementary materials and methods)

confirming the T cell phenotype by staining CD3 and CD8. Finally, 10^7 CD8$^+$ T cells in sterile PBS were injected i.v. into C57BL/6 mice 12 hours prior to inoculation with 10^6 C1498/GFP AML cells.

2.5.9 Xenotransplantation of human PBMCs into NSG mice

Human PBMCs were extracted from whole blood by density gradient centrifugation as described in 2.2.5 and frozen at -80°C. When due for *in vivo* studies, the cells were thawed, washed with sterile PBS three times and injected into NSG mice via the tail vein at a number of 10^7 cells per mouse using an injection volume of 200 µl PBS.

2.6 Statistical analysis[8]

Statistical analyses were performed with GraphPad Prism versions 7.0c and 9.3.0. Data were analyzed using the unpaired Student's t-test if data sets of different time points were compared or if treatment responses between different groups were assessed at a given time point. One-way ANOVA was used to calculate statistical differences between different genotypes at one time point. Overall survival was compared by log-rank test. The tests applied are indicated in the respective figure legends. Hazard ratios stated were calculated applying the Mantel-Haenszel method. n-values reflect total numbers of mice if data derive from pooled experiments. Results were considered statistically significant at values of $p < 0.05$. p values are indicated by n. s. for not significant, * for $p < 0.05$, ** for $p < 0.01$, *** for $p < 0.001$ and **** for $p < 0.0001$.

---

[8] With some modifications as described in Ruzicka, Koenig et al. 2020 (Supplementary materials and methods)

3. Results

3.1 Systemically administered ppp-RNA decreases AML burden *in vivo*, delays AML progression and leads to long-term survival[9]

The following *in vivo* experiments investigate the effect of systemic immunotherapy with ppp-RNA on AML progression in the syngeneic C1498 mouse model.

3.1.1 *In vivo* growth analysis of the C1498/GFP AML cell line

C1498 is a murine AML cell line with C57BL/6 background classified as acute myelomonocytic leukemia (Mopin et al. 2016). *In vivo*, it displays aggressive growth with infiltration of various organ systems, including the bone marrow, blood, spleen, liver, lungs and ovaries (data not shown). After inoculation, mice appear asymptomatic for 15-20 days. First signs of disease are commonly followed by rapid progression.

Manual intravenous injections in mice are a delicate matter requiring high precision from the experimenter, inevitably resulting in slight dose variance during the process of tumor inoculation. After the C1498 AML model was established in our laboratory, I investigated how much of an effect a varying dose of injected tumor cells would have on disease progression and thus the outcome of my *in vivo* experiments. Therefore, I injected two C57BL/6 wild type (WT) mice per group with either 10^6, 5×10^5 or 2.5×10^5 green fluorescent protein (GFP) expressing C1498 AML cells (C1498/GFP). No further treatment was applied and the mice were sacrificed when the criteria for termination were met. Interestingly, the cell numbers used for leukemia induction did not significantly affect disease progression (median survival of 18 days for mice receiving 1×10^6 cells vs. 18 days for mice receiving 5×10^5 cells ($p > 0.999$) vs. 19 days for mice receiving 2.5×10^5 cells ($p = 0.317$); Figure 1), making the process of manual injections an unlikely source of bias in the *in vivo* experiments to follow.

---

[9] Results as described in Ruzicka, Koenig et al. 2020 with some modifications
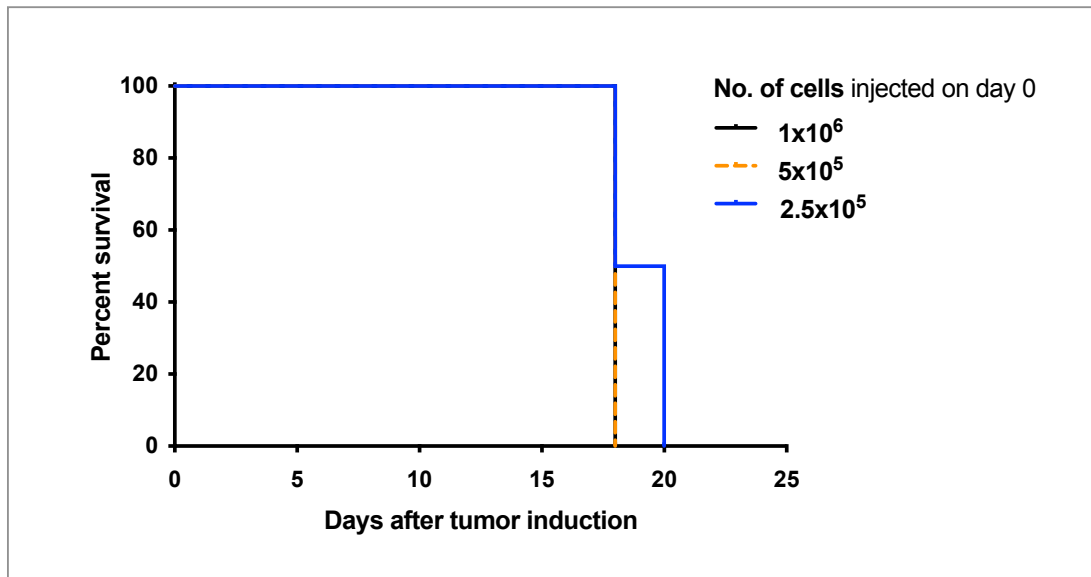
Figure 1. Growth analysis of the C1498/GFP AML tumor cell line *in vivo*. C57Bl/6 mice (n = 2 per group) were inoculated with either 10^6, $5x10^5$ or $2,5x10^5$ C1498/GFP AML cells. No further treatment was applied. Mice were sacrificed at signs of disease onset and survival data were plotted in a Kaplan-Meier survival curve.

3.1.2 ppp-RNA treatment decreases the AML tumor burden in C1498/GFP AML-bearing mice

In order to investigate the overall therapeutic potential of systemic ppp-RNA treatment of AML, I inoculated C57BL/6 mice with $1x10^6$ C1498/GFP cells via tail vein injection. 50 µg of *in vivo*-jetPEI-complexed ppp-RNA were administered intravenously on days 3, 7, 10 and 14 after tumor inoculation (Figure 2A). Mice were sacrificed on day 17, and the tumor burden in blood, bone marrow, livers, lungs, ovaries and spleens was measured via flow cytometry. I found significantly reduced tumor mass in bone marrow (2,1% vs. 18,1% GFP positive cells for ppp-RNA treated (n = 3) vs. untreated mice (n = 5), p = 0.002; Figure 2B), lungs (3,6% vs. 68,8% GFP positive cells for ppp-RNA treated (n = 3) vs. untreated mice (n = 5), p < 0.001), ovaries (0.5% vs. 45,3% GFP-positive cells for ppp-RNA treated (n = 3) vs. untreated mice (n = 4), p = 0.004), and spleens (0.03% vs. 12.6% GFP positive cells for ppp-RNA treated (n = 3) vs. untreated mice (n = 5), p = 0.009).
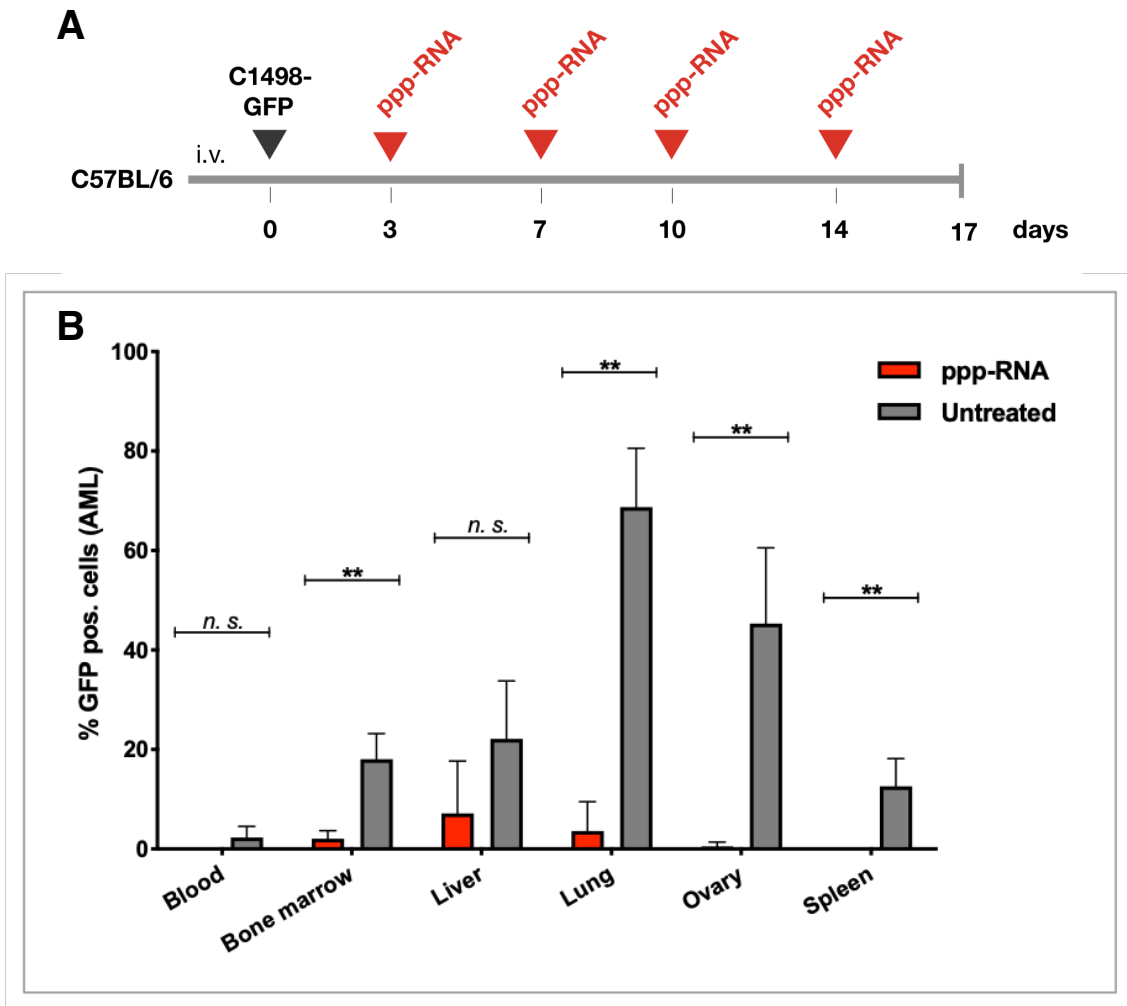
Figure 2. Tumor load in indicated organs after systemic ppp-RNA treatment of C1498/GFP AML-bearing mice. C57BL/6 mice were inoculated with 1×10^6 C1498/GFP AML cells and treated with 50 µg of ppp-RNA as depicted in (A). (B) ppp-RNA-treated (bar charts indicate mean of n = 3 with SEM) and untreated (bar charts indicate mean of n = 5 with SEM) C57BL/6 mice were sacrificed on day 17. Single cell suspensions of blood, bone marrow, livers, lungs, ovaries and spleens were analyzed by flow cytometry determining the fraction of GFP positive cells (AML cells). Statistical significance was determined using Student's t-test (B) with comparisons indicated by brackets. Figure and figure legend modified from Ruzicka, Koenig et al. 2020.

3.1.3 ppp-RNA treatment prolongs survival of C1498/GFP AML-bearing mice

Next, I focused on the potential effects of systemic RIG-I activation on the survival of AML-bearing mice. C57BL/6 mice were inoculated with 1×10^6 C1498/GFP AML cells and treated with ppp-RNA adhering to the scheme shown in *Figure 2A*. Animals were sacrificed at signs of disease onset and survival data were plotted

in a Kaplan-Meier survival curve (Figure 3). The onset of symptomatic AML
disease appeared significantly delayed (median survival 26 days vs. 18 days with
$p < 0.0001$ for ppp-RNA treated (n = 16) vs. untreated mice (n = 16)). In addition,
the treatment led to long-term remission in 3 out of 16 (19%) of the animals,
demonstrating the potential of systemic ppp-RNA therapy in AML.
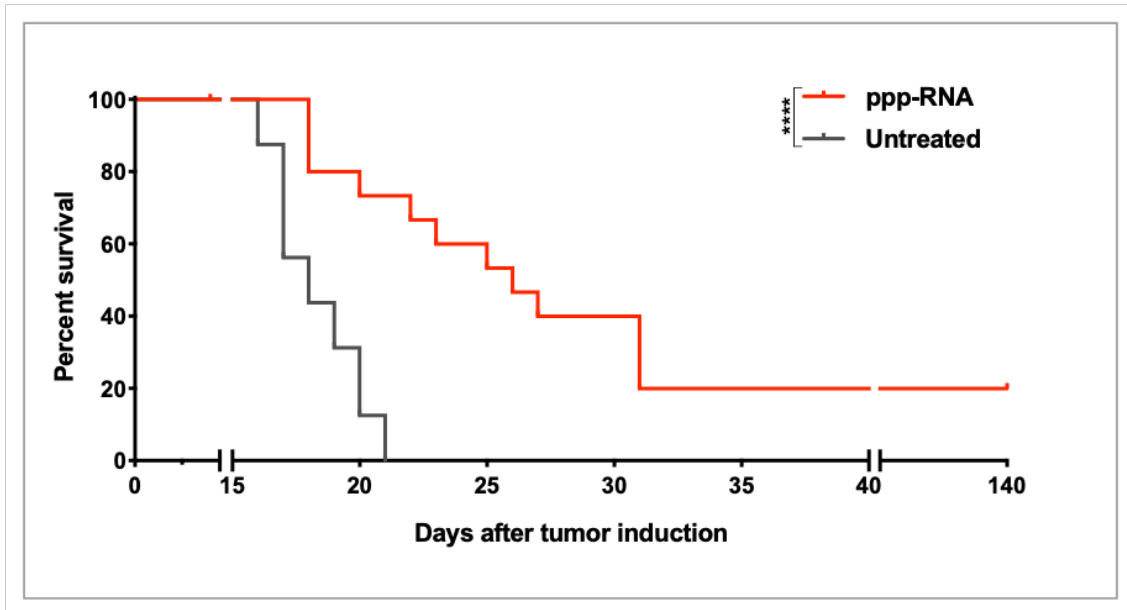

Figure 3. Survival of ppp-RNA-treated C1498/GFP AML-bearing mice. C1498/GFP AML was
induced in C57BL/6 mice (n = 16 per group) and ppp-RNA therapy was applied according to the
scheme in *Figure 2A*. Survival data were plotted in a Kaplan-Meier survival curve and statistical
significance was calculated with log-rank test. Figure and figure legend modified from Ruzicka,
Koenig et al. 2020.

3.1.4 Treatment effects are not limited to GFP-expressing C1498 AML cells

Recent studies have revealed that GFP expression may enhance the
immunogenicity of affected cells while diminishing their lifetime (Ansari et al.
2016). To assess the role of GFP as a potentially immunogenic target in my
model, C57BL/6 mice were inoculated with 1×10^6 C1498 wild type (WT) cells and
treated with ppp-RNA according to the scheme in *Figure 2A*. The results show
persistent extension of disease-free lifetime in the treated group compared to
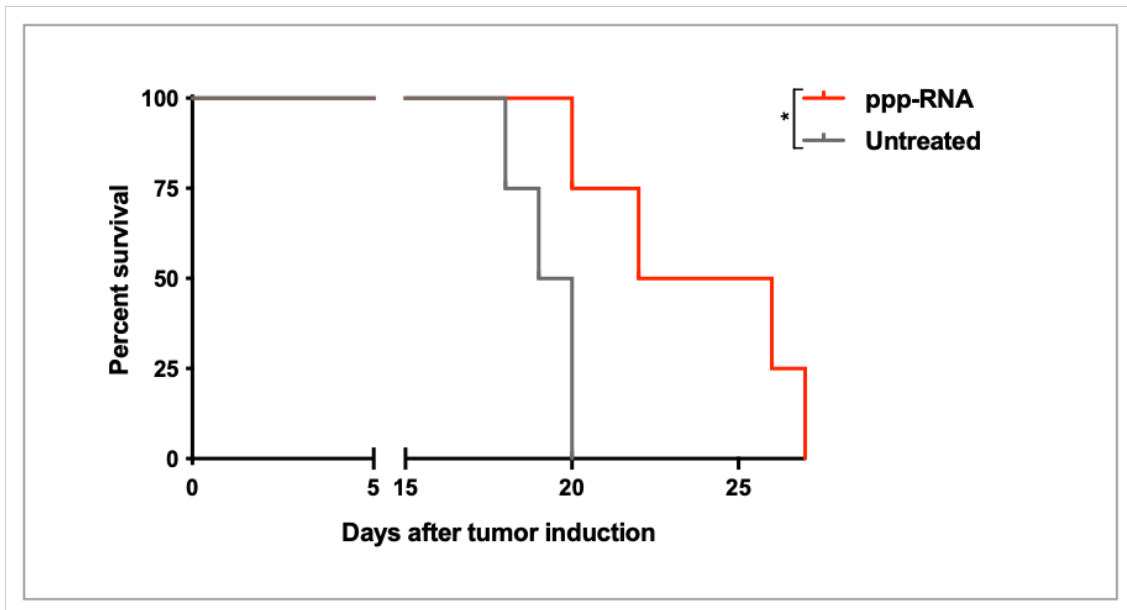untreated mice (p = 0.029, Figure 4).

Figure 4. Survival of ppp-RNA treated C1498 WT AML-bearing mice. C1498 WT AML was induced in C57BL/6 mice (n = 4 per group) and ppp-RNA therapy was applied according to the scheme in *Figure 2A*. Survival data were plotted in a Kaplan-Meier survival curve and statistical significance was calculated with log-rank test.

3.2 Treatment efficacy of ppp-RNA depends on adaptive cellular immunity, intact IFNAR and MAVS signaling in the host[10]

The following chapter focuses on identifying the mechanisms responsible for the ppp-RNA-mediated tumor rejection of C1498 AML cells that I observed previously.

3.2.1 ppp-RNA treatment effect is dependent on adaptive immunity

The C1498/GFP AML cell line resists transfection with most commercially available RNA transfection reagents *in vitro* (data not shown). In order to discriminate between a direct cytotoxic effect on the tumor cell as described before (Besch et al. 2009) and an immune-cell-mediated response, I used immune-deficient NSG mice lacking T, B and NK cells. The mice were inoculated with C1498/GFP AML cells and ppp-RNA treatment was given on days 3, 6, 9

---

[10] Results as described in Ruzicka, Koenig et al. 2020 with some modifications

and 12. Both treated and untreated animals died on day 13 (Figure 5). Further, no significant differences regarding tumor burden were detected between the two groups via flow cytometry in various organs (data not shown), demonstrating a lack of ppp-RNA treatment efficacy in the absence of adaptive immune cells.
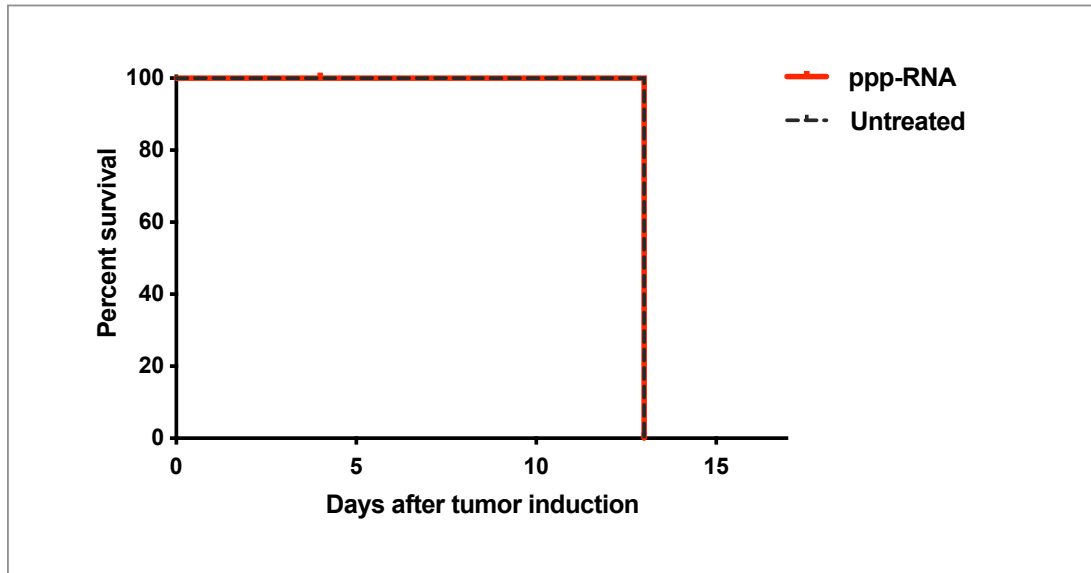

Figure 5. ppp-RNA induced tumor rejection is mediated by cellular immunity. NSG mice (n = 5 per group) were inoculated with C1498/GFP AML cells and ppp-RNA therapy was applied on days 3, 6, 9 and 12. Survival data were plotted in a Kaplan-Meier survival curve.

3.2.2 CD4$^+$ and CD8$^+$ T cells mediate ppp-RNA induced AML rejection

Learning about the critical role the adaptive immune system plays in the ppp-RNA-mediated immune response against AML cells, I next decided to investigate which immune cell types in particular were involved. I chose to specifically deplete CD4$^+$ or CD8$^+$ T cells, CD19$^+$ B or NK1.1$^+$ NK cells in ppp-RNA treated, C1498/GFP AML-bearing C57BL/6 mice and compared the survival curves. While CD8$^+$ (p = 0.003) and CD4$^+$ T cell (p = 0.018) depleted mice showed significantly impaired survival (Figure 6A), depletion of CD19$^+$ (p = 0.401) and NK1.1$^+$ (p = 0.376) cells remained without significant effect compared to the respective isotype controls (Figure 6B). These findings suggest that CD4$^+$ and CD8$^+$ T cells are central mediators of the ppp-RNA-induced antileukemic immune response.
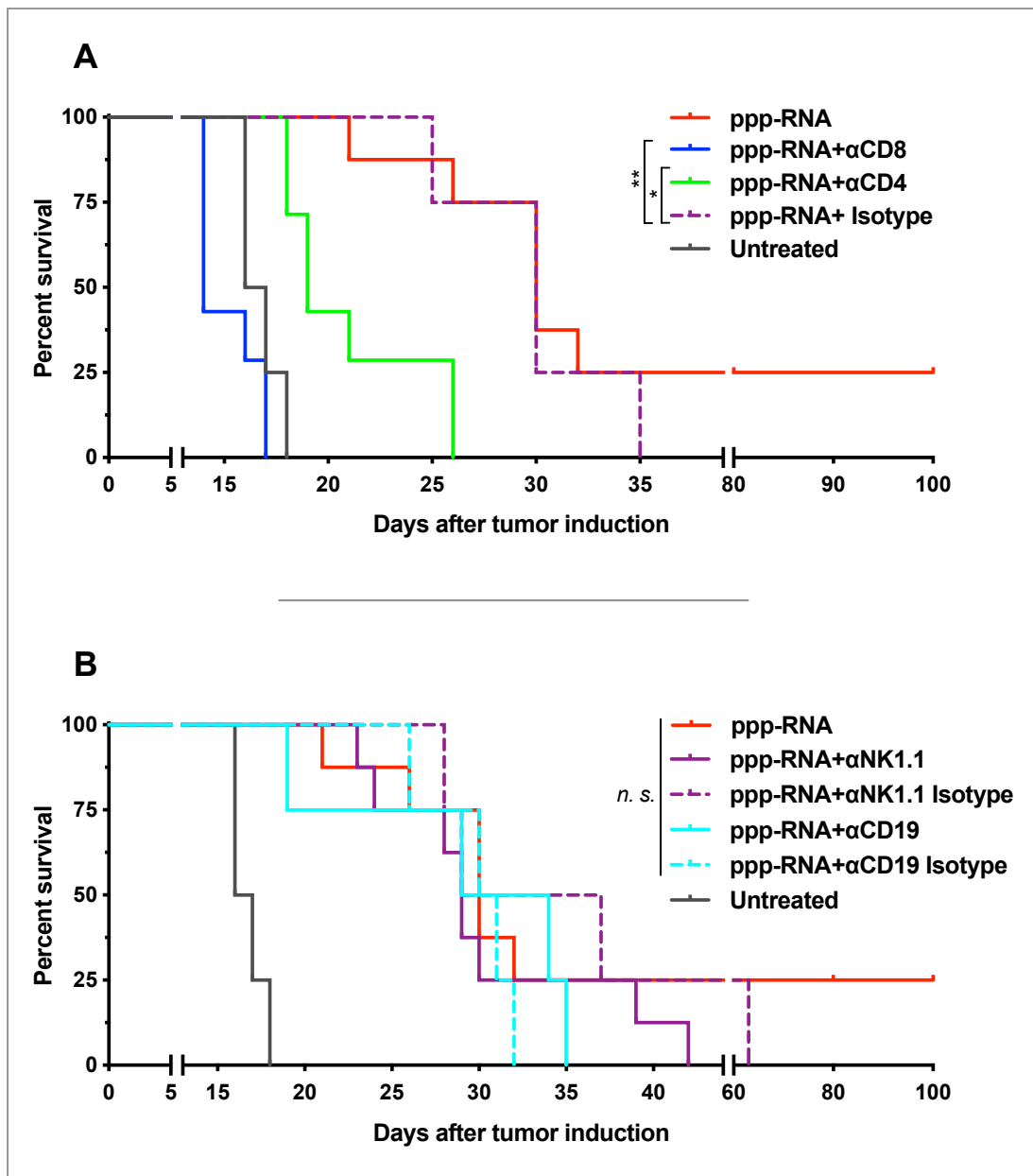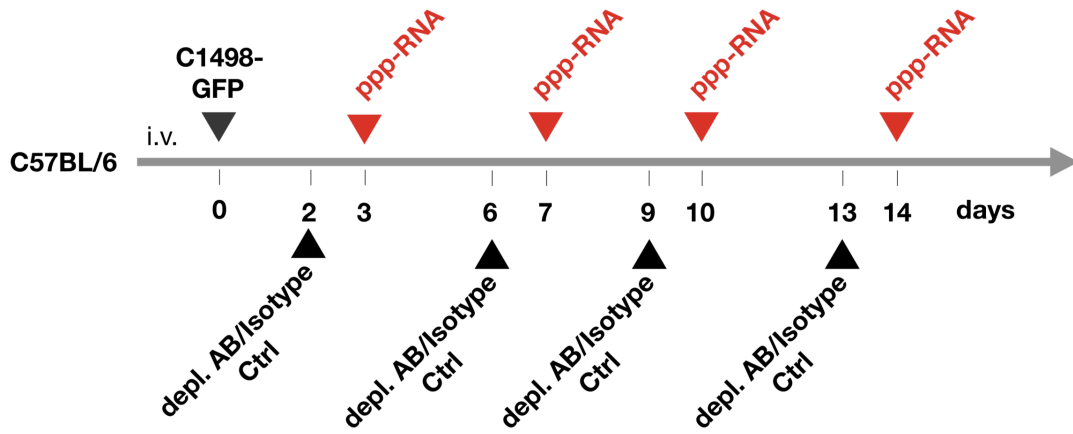
Figure 6. ppp-RNA induced tumor rejection is mediated by adaptive immune cells. (A, B)
C57BL/6 mice were inoculated with C1498/GFP AML cells and therapy was applied as displayed

above (n = 7 per group for ppp-RNA treated mice, n = 8 for untreated mice, n = 4 for ppp-RNA + αCD19 treated mice). Depleting antibodies (AB) were administered as described in materials and methods. Corresponding isotype controls were tested in a total of n = 4 mice per group. Survival data were plotted in two Kaplan-Meier survival curves. p values of immune cell depleted groups compared to respective isotype controls were calculated using log-rank test: $p = 0.018$ for CD4+, $p = 0.003$ for CD8+, $p = 0.376$ for NK1.1+, $p = 0.401$ for CD19+ cell depletion. Figure and figure legend modified from Ruzicka, Koenig et al. 2020.

3.2.3 Intact IFNAR and MAVS signaling in the host organism are essential for long-term remission

Previously, several other PRRs have been described to directly or indirectly sense short double-stranded and hairpin RNAs, resulting in type I IFN induction (Schlee et al. 2016), similarly to RIG-I. To determine the contribution of off-target effects on the therapeutic outcome of ppp-RNA treatment and to further evaluate the role of RIG-I signaling in the host, I compared the effects of ppp-RNA treatment in C57BL/6 WT, MAVS- and IFNAR1-deficient mice. The treatment was applied as depicted in *Figure 2A*.

3.2.3.1 Repeated ppp-RNA treatment in *Mavs*-/- and *Ifnar1*-/- mice fails to induce CXCL10

First, I sought to evaluate the immunostimulatory activity of ppp-RNA in *Mavs*-/- and *Ifnar1*-/- mice. CXCL10 serum levels were measured via ELISA after the first and fourth treatment with ppp-RNA, serving as a surrogate marker for type I IFN release. In WT and *Mavs*-/- mice, the treatment resulted in comparable serum levels of CXCL10 four hours after the first treatment ($p = 0.986$ for WT vs. *Mavs*-/- mice; Figure 7), while in *Ifnar1*-/- mice only very low levels of CXCL10 were measured after both treatments. Interestingly, CXCL10 levels four hours upon the fourth ppp-RNA treatment in *Mavs*-/- mice dropped significantly while CXCL10 levels measured in WT mice remained constant ($p = 0.469$ for first vs. fourth treatment in WT mice, $p = 0.001$ for first vs. fourth treatment in *Mavs*-/- mice and $p < 0.001$ for WT vs. *Mavs*-/- mice after fourth treatment; Figure 7).
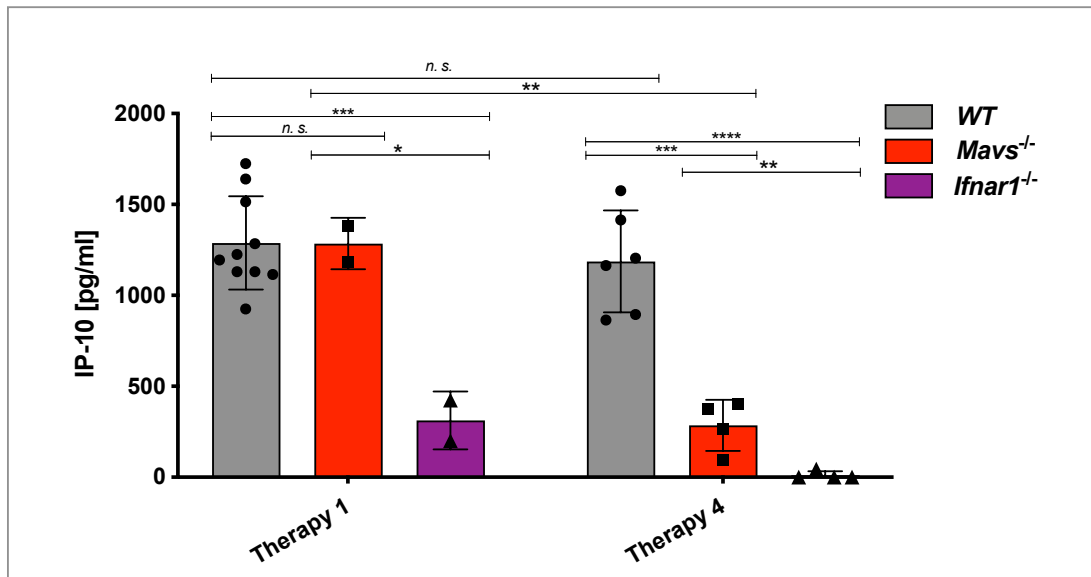
Figure 7. Immunostimulatory activity of ppp-RNA in WT, *Mavs*-/- and *Ifnar1*-/- mice. C57BL/6 WT, *Mavs*-/- and *Ifnar1*-/- mice were treated with 50 µg of ppp-RNA on days 3, 7, 10 and 14 after inoculation with C1498/GFP AML cells as shown in *Figure 2A*. Blood was drawn after the first (day 3) and fourth (day 14) treatment and levels of murine CXCL10 were measured via ELISA. Each symbol represents a single mouse and error bars indicate standard deviation (SD). Statistical differences between genotypes at one time point were determined by one-way ANOVA with Tukey's post-hoc test and differences of individual groups between time points with Student's t-test. Figure and figure legend modified from Ruzicka, Koenig et al. 2020.

3.2.3.2 ppp-RNA treatment in *Mavs*-/- mice prolongs survival, but fails to establish long-term remission

Next, I assessed how these findings would reflect on the survival of the respective mice. Despite dysfunctional RIG-I downstream signaling, *Mavs*-/- mice still significantly benefitted from ppp-RNA treatment with regard to overall survival (p = 0.0193 for ppp-RNA treated vs. untreated mice; Figure 8). Nevertheless, the effect was less pronounced than in WT mice (see Figure 3; hazard ratios for ppp-RNA treated vs. untreated mice: 0.229 in *Mavs*-/- vs. 0.113 in WT mice). Of note, no long-term survival was observed in *Mavs*-/- mice. Taken together, intact RIG-I signaling via MAVS in the host organism seems to be crucial particularly for repeated ppp-RNA treatment and long-term remission.
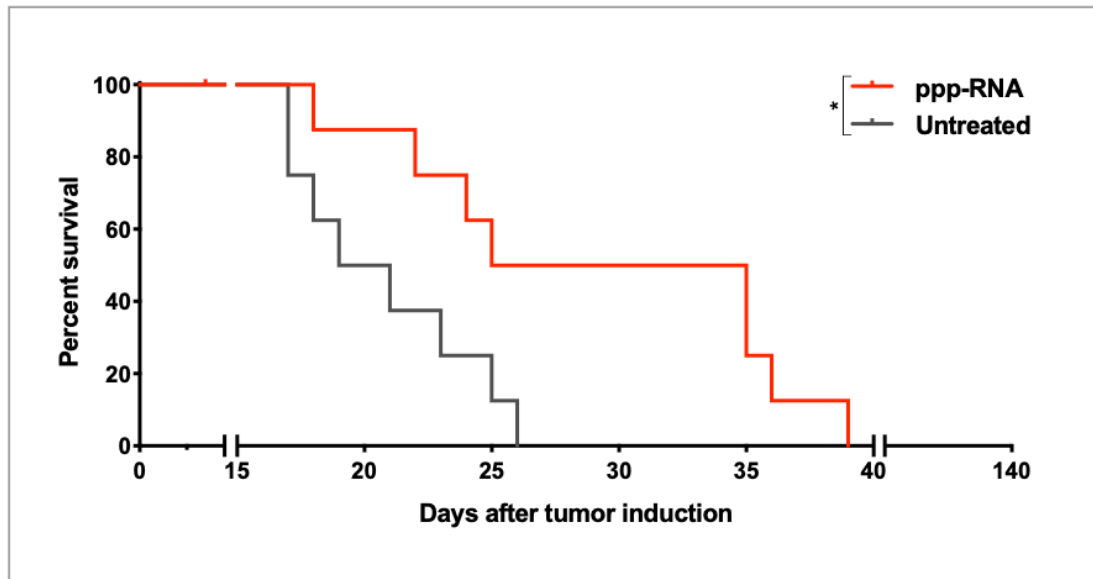
Figure 8. ppp-RNA treatment in C1498/GFP AML-bearing *Mavs*^-/- mice. C57BL/6 *Mavs*^-/- mice (n = 9 per group) were inoculated with C1498/GFP AML cells and treated with 50 µg of ppp-RNA on days 3, 7, 10 and 14 as depicted in *Figure 2A* or left untreated. Survival data were plotted in a Kaplan-Meier survival curve. Figure and figure legend modified from Ruzicka, Koenig et al. 2020.

3.2.3.3 Intact IFNAR signaling in the host organism is crucial for ppp-RNA treatment efficacy

In *Ifnar1*^-/- mice, the treatment failed to delay disease progression (p = 0.073 for ppp-RNA vs. untreated mice, median survival of 17 days vs. 15.5 days for ppp-RNA treated vs. untreated mice; Figure 9A), accentuating the role of intact type I IFN signaling in the context of ppp-RNA treatment. This raised the question as to whether type I IFN alone may mediate the therapeutic effects I observed so far. I therefore applied a therapeutic dose of murine IFNα i.p. to C1498/GFP AML-bearing mice on days 3, 7, 10 and 14. IFNα alone failed to prolong the overall survival of mice (p = 0.352 for IFNα treated vs. untreated mice, median survival of 16 days vs. 15 days for IFNα treated vs. untreated mice; Figure 9B), suggesting that within my model, the immune response induced by ppp-RNA is critically dependent on, but not limited to the effects of IFN type I release.
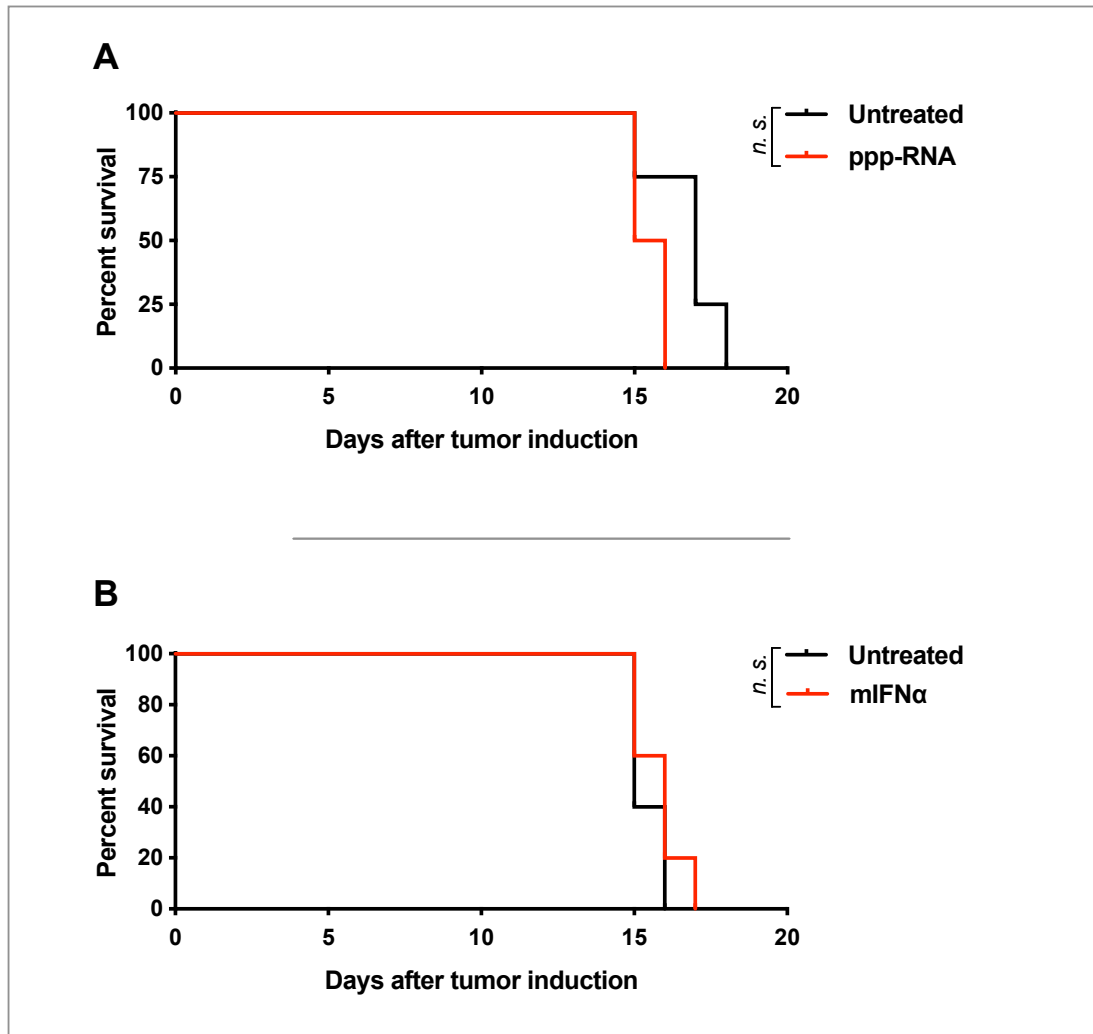
Figure 9. ppp-RNA treatment depends on intact IFNα signaling. (A) *Ifnar1-/-* mice (n = 4 per group) were inoculated with C1498/GFP AML cells and treated according to the scheme depicted in *Figure 2A*. Survival data were plotted in a Kaplan-Meier survival curve. p = 0.073 for ppp-RNA vs. untreated mice. (B) C1498/GFP AML-bearing C57BL/6 WT mice (n = 10) were randomized into two groups, one of which received 5x10⁴ IU murine IFN alpha (mIFNα) i.p. on days 3, 7, 10 and 14. Survival data were plotted in a Kaplan-Meier survival curve. p = 0.352 for mIFNα treated vs. untreated mice. Figure and figure legend modified from Ruzicka, Koenig et al. 2020.

3.3 ppp-RNA treatment induces immunological memory formation[11]

3.3.1 ppp-RNA treated, AML surviving mice are protected against rechallenges with C1498/GFP AML cells

Next, I decided to investigate if in ppp-RNA treated mice that have achieved long-term AML remission, a long-lasting immunological memory was formed. Surviving mice were rechallenged with a single dose of C1498/GFP AML cells on day 85 to 110 after the first AML inoculation. Tumor-naïve mice served as control animals and were inoculated with the identical number of C1498/GFP AML cells. Survivor mice withstood the AML rechallenge in all cases (n = 7 for AML surviving vs. n = 10 for tumor-naïve mice, p < 0.0001; Figure 10).
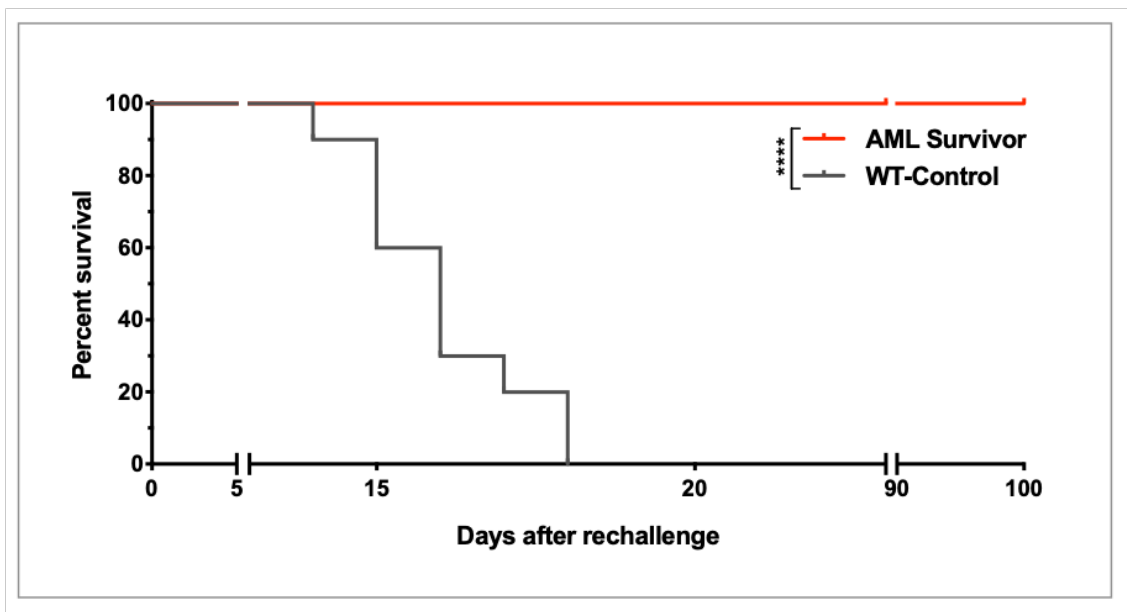
Figure 10. Tumor rechallenge of C1498/GFP AML surviving mice. C1498/GFP AML surviving C57BL/6 mice (n = 7) were rechallenged with $1x10^6$ C1498/GFP AML cells i.v. No further treatment was applied. Tumor-naïve C57BL/6 mice (n = 10) served as controls and received the identical number of AML cells. Survival data were plotted in a Kaplan-Meier survival curve. Significance was calculated using log-rank test. Figure and figure legend modified from Ruzicka, Koenig et al. 2020.

---

[11] Results as described in Ruzicka, Koenig et al. 2020 with some modifications

3.3.2 Immunological memory responses are partially mediated by CD8+ T cells

Seeking to identify the cellular mediators of the memory responses I observed, I adoptively transferred CD8+ T cells from survivor mice into WT recipient C57BL/6 mice. 12 hours after the adoptive transfer, the mice were inoculated with C1498/GFP AML cells. CD8+ T cells from tumor-naïve C57BL/6 mice served as control. I observed significantly prolonged survival in mice treated with CD8+ T cells derived from ppp-RNA treated, AML surviving mice compared to tumor-naïve donors (p = 0.007; Figure 11). Although protection from disease progression does not seem to be infinite, these findings do indicate a central role of CD8+ T cells as mediators of the immunological memory responses I observed.
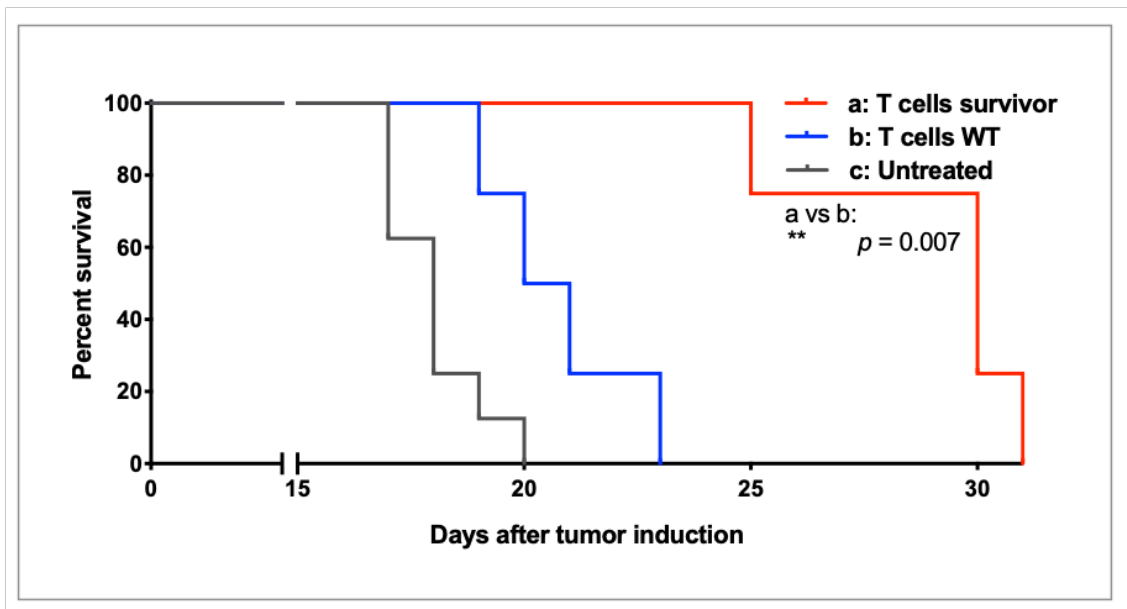
Figure 11. Adoptive transfer of CD8+ T cells from AML surviving into AML naïve, then C1498/GFP inoculated mice. C57BL/6 mice (n = 4) were treated with CD8+ T cells from C1498/GFP AML surviving (T cells survivor, n = 3) or tumor-naïve mice (T cells WT, n = 5), respectively. Untreated mice (n = 8) served as controls. C1498/GFP AML was induced 12 hours later in all three groups. T cells were isolated and expanded as described in materials and methods. Survival data were plotted in a Kaplan-Meier survival curve. Significance was calculated using log-rank test. Figure and figure legend modified from Ruzicka, Koenig et al. 2020.

3.4 ppp-RNA treatment leads to PD-L1 upregulation on AML cells *in vivo* and induces sensitivity to anti-PD-1 checkpoint inhibition therapy[12]

Learning about the essential role intact IFN signaling plays in ppp-RNA-mediated rejection of C1498/GFP AML cells (see Figures 7, 9A), I decided to explore if in this particular model of AML therapeutic targeting of the PD-1/PD-L1 axis would lead to synergistic results.

3.4.1 ppp-RNA treatment induces PD-L1 upregulation on C1498/GFP AML cells *in vitro* and *in vivo*

First, I assessed if PD-L1 expression on C1498/GFP AML cells was IFN inducible. I therefore seeded the cells *in vitro* and stimulated them with IFNγ, which led to strong upregulation of PD-L1 on the tumor cells ($p < 0.001$ for IFNγ treated vs. untreated cells; Figure 12A).

Next, PD-L1 expression *ex vivo* was measured. I focused on AML cells infiltrating lung tissue of C57BL/6 mice, as in this organ I previously observed the strongest effects of ppp-RNA treatment on tumor loads (see Figure 2B). Mice were treated with ppp-RNA and sacrificed 12 hours thereafter. Flow cytometry analysis of lung tissue showed significantly higher expression of PD-L1 on C1498/GFP AML cells after treatment ($p = 0.002$; Figure 12B).

---

[12] Results as described in Ruzicka, Koenig et al. 2020 with some modifications
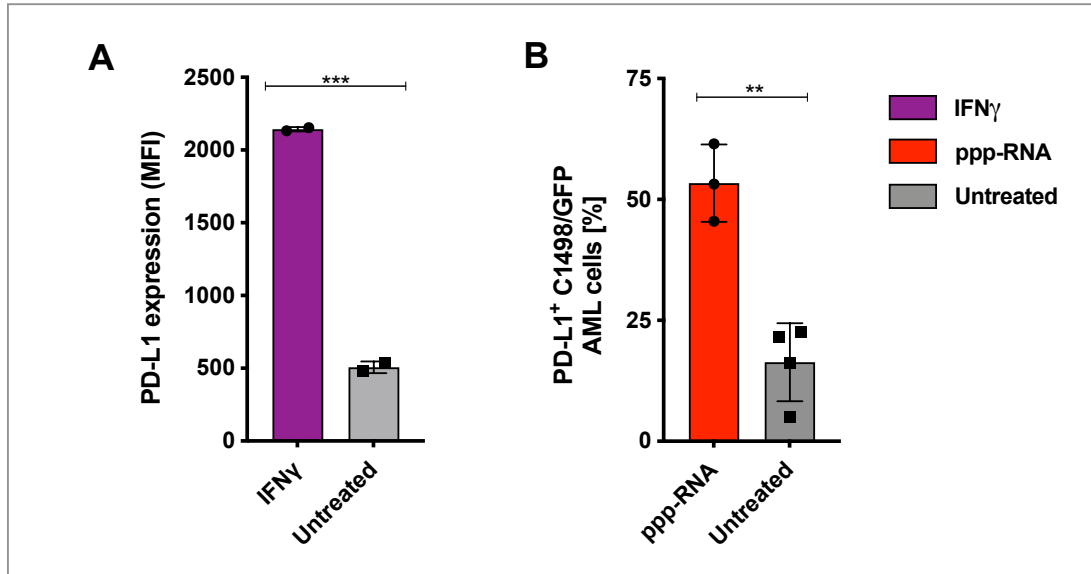
Figure 12. PD-L1 expression on C1498/GFP AML cells *in vitro* and *in vivo* after treatment.
(A) 2.5×10^5 C1498/GFP AML cells were seeded in 6-well format and treated with IFNγ. PD-L1 expression was determined by flow cytometry 72 hours after stimulation. (B) C1498/GFP AML-bearing C57BL/6 mice received three treatments of 50 µg ppp-RNA on days 8, 11 and 14 after tumor induction. 12 hours upon the last treatment (day 15), mice were sacrificed and single cell suspensions of lung tissue were analyzed by flow cytometry, determining PD-L1 expression on GFP positive AML cells. Dots and squares represent individual animals. Statistical significance was determined by Student's t-test (A, B). Figure and figure legend modified from Ruzicka, Koenig et al. 2020.

3.4.2 Treatment with ppp-RNA and anti-PD-1 antibody shows augmented efficacy

To evaluate if these findings had any therapeutic implications, I chose to treat C1498/GFP AML-bearing C57BL/6 mice with ppp-RNA following the regular treatment scheme, using a suboptimal dose of 25 µg RNA. Additionally, I applied 100 µg of anti-PD-1 blocking antibody i.p. on days 6, 9 and 13 (see treatment scheme depicted in *Figure 13*). 4 hours after the first ppp-RNA treatment (day 3), I measured serum levels of murine CXCL10 (Figure 13A). The results demonstrate even immunostimulatory activity of the treatment among the two groups receiving ppp-RNA (p = 0.21 for ppp-RNA treated vs. ppp-RNA + anti-PD-1 antibody treated mice).

Comparison of the survival curves, in contrast, demonstrates that combined treatment with ppp-RNA plus the anti-PD-1 antibody was superior to either of the therapeutic agents applied alone (p = 0.02; Figure 13B). Further, mice treated with only the anti-PD-1 antibody showed no survival benefit at all if compared to untreated animals, indicating that ppp-RNA is necessary to prime AML cells for efficient checkpoint inhibition (p < 0.001 for ppp-RNA + αPD-1 vs. αPD-1 treated mice).

In a next step, the dose of ppp-RNA was increased to 50 μg while the dose of anti-PD-1 antibody was kept constant (Figure 13 C). The results indicate higher efficacy, yet fail to achieve statistical significance, showing a trend towards increased long-term survival of above 30% in the group treated with both ppp-RNA and anti-PD-1 blocking antibody (p = 0.274 for ppp-RNA + αPD-1 vs. ppp-RNA only).
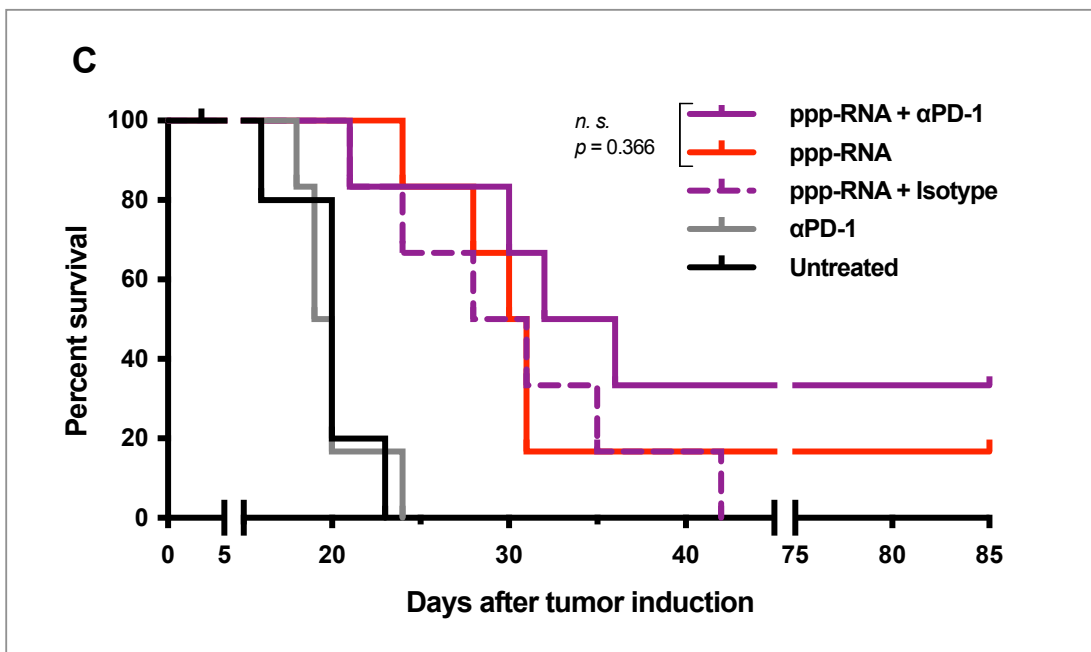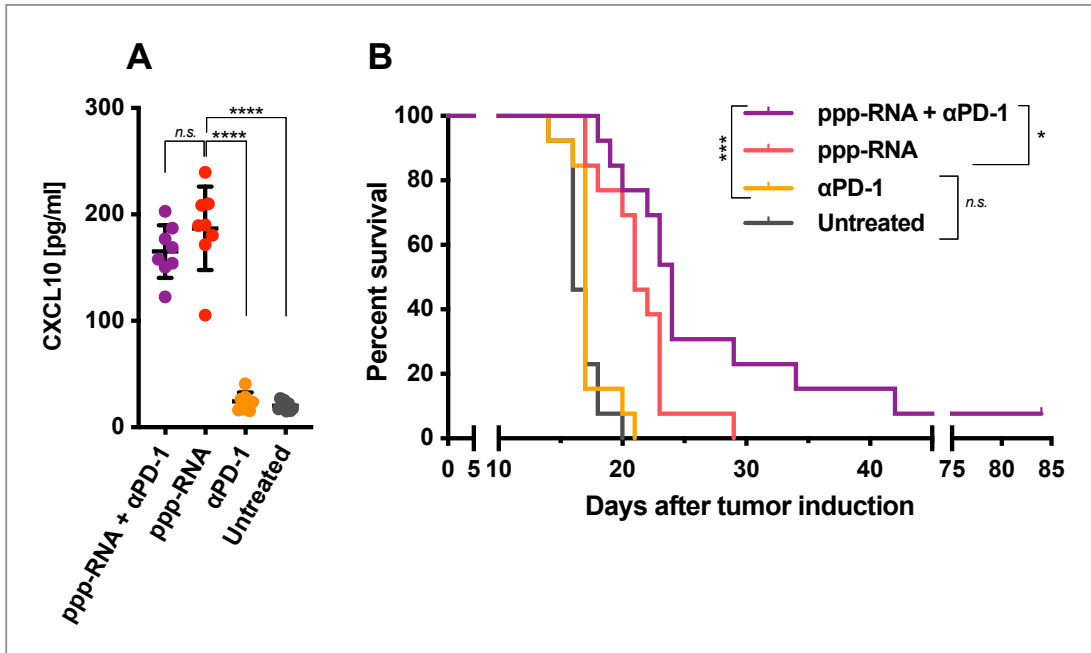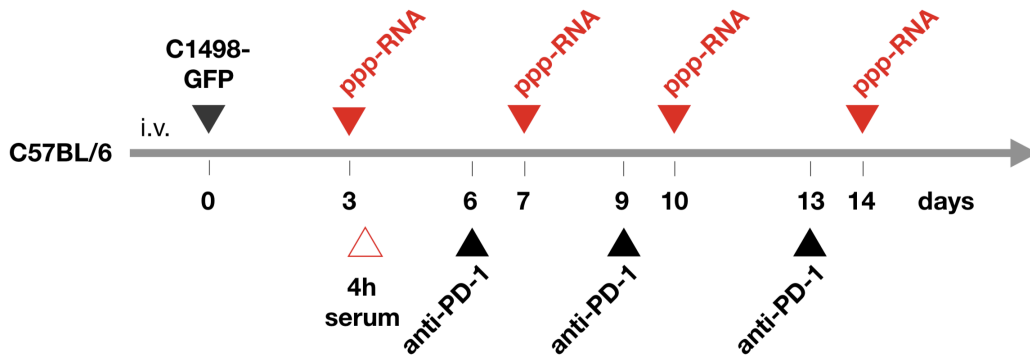
Figure 13. ppp-RNA treatment primes AML cells for anti-PD-1 checkpoint inhibition. (A, B, C) C57BL/6 mice (n = 13 per group (A, B), n = 6 per group (C)) were inoculated with C1498/GFP AML cells on day 0 and treated with 25 µg (or 50 µg, respectively, Figure 13C) of ppp-RNA on days 3, 7, 10 and 14. 100 µg of anti-PD-1 antibody (αPD-1) were injected i.p. on days 6, 9 and 13. Levels of murine CXCL10 were determined by ELISA in blood serum obtained 4 hours after the first treatment with 25 µg of ppp-RNA (n = 8 per group) (A). Survival data were plotted in a Kaplan-Meier survival curve (B, C). Statistical significance was determined by one-way ANOVA with Tukey's post-hoc test (A) and log-rank test (B, C). Figure and figure legend modified from Ruzicka, Koenig et al. 2020.

3.5 ppp-RNA therapy in a humanized mouse model of AML

Evaluating the potential of ppp-RNA-based immunotherapy for clinical translation, I established an immune reconstituted humanized mouse model of AML using PDX AML cells (Ruzicka et al. 2020). The cells were produced by serial retransplantation of primary patient leukemic cells in NSG mice and their growth kinetics *in vivo* were previously described (Vick et al. 2015). Therefore, I first focused on studying the dynamics of human PBMCs xenografted into NSG mice. Instead of Human Leukocyte Antigen (HLA) matching, I prioritized to empirically identify a donor whose cells would xenoreact with the murine host organism minimally, thus granting me a greater time window for the experiments.

3.5.1 *In vivo* growth analysis of human PBMCs

A total of six NSG mice were randomized into three groups, each group receiving 1×10^7 human PBMCs from a different healthy human donor. I analyzed peripheral blood by flow cytometry and determined the fraction of human cells over time. While at day 6, human PBMCs only made up 1% of the white blood cells, from day 10 on, the cells showed strong expansion, eventually reaching a frequency of above 50% (Figure 14A). Over time, the mice started to show initial signs of graft-versus-host-disease (GvHD), thus meeting criteria for termination. The survival data (Figure 14B) reveal that the time point of GvHD onset is donor

dependent. According to the needs mentioned above, donor II was chosen for the further experiments.
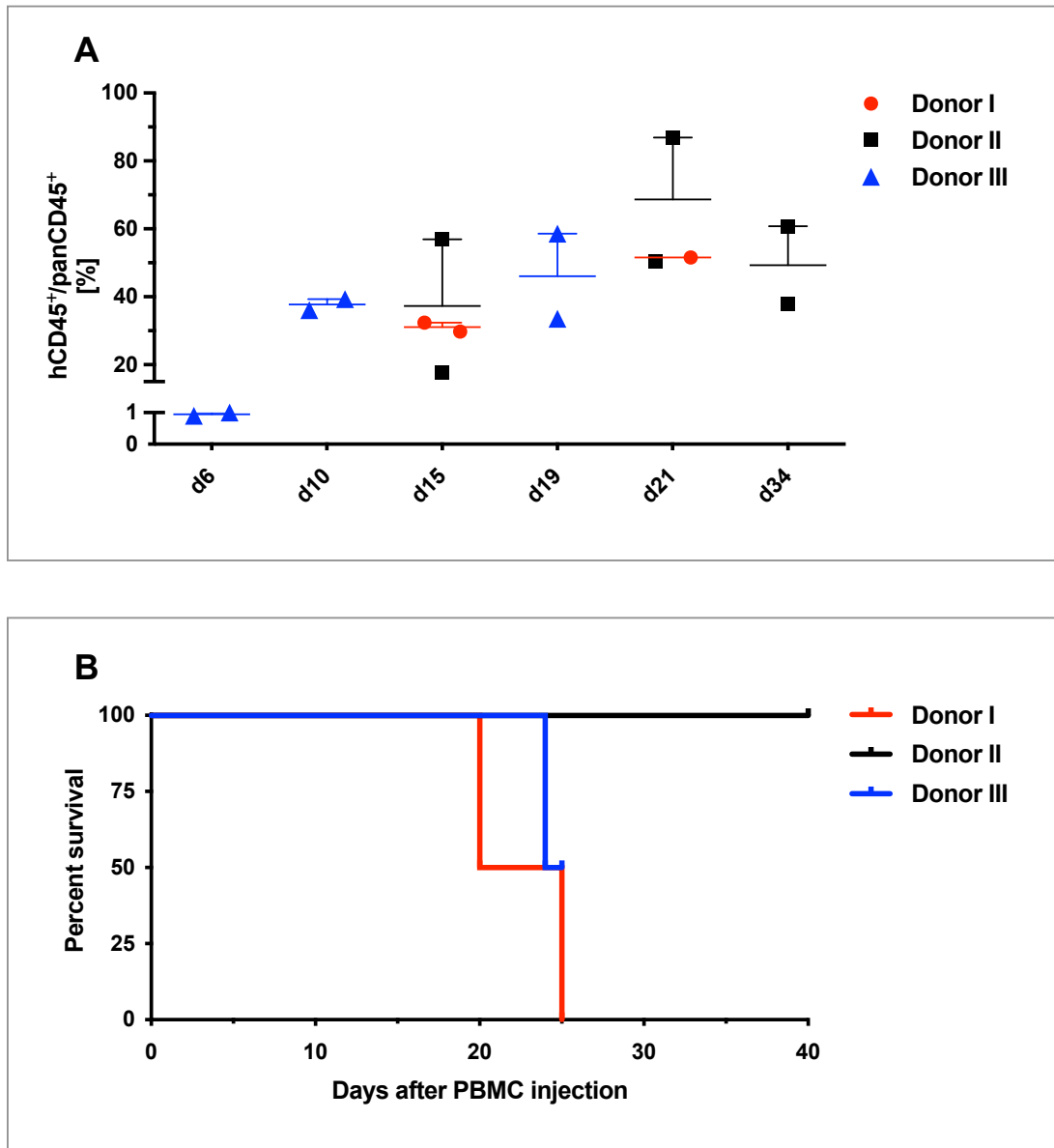
Figure 14. Engraftment and growth of human PBMCs xenotransplanted into NSG mice. (A, B) NSG mice (n = 2 per group) were injected with human PBMCs of three different donors at day 0. (A) The fraction of human CD45 positive (hCD45$^+$) cells was determined via flow cytometry and plotted as percent of murine CD45 positive (mCD45$^+$) plus hCD45$^+$ cells (panCD45$^+$). (B) The mice were monitored and sacrificed at onset of GvHD. Survival data were plotted in a Kaplan-Meier survival curve.

3.5.2 ppp-RNA treatment reduces the AML burden in a humanized mouse model of AML[13]

To assess the therapeutic potential of ppp-RNA treatment in a humanized, preclinical setting, NSG mice were inoculated with 4.5×10^5 PDX AML 491 cells via the tail vein. Disease progression was monitored regularly by flow cytometry, measuring the fraction of PDX AML 491 cells in the peripheral blood. Once an average tumor load of 51% in the peripheral blood was achieved (day 52, data not shown), all animals received 10^7 human PBMCs from donor II via tail vein injection.

Consecutively, 50 µg of ppp-RNA were administered thrice in total (days 53, 56 and 59). On day 60, the animals were sacrificed. The AML burden and immune cell numbers were determined by flow cytometry in peripheral blood and bone marrow (Figure 15A, B). In both blood ($p < 0.001$) and bone marrow (n.s., $p = 0.071$), ppp-RNA treated animals exhibited a lower AML burden than untreated animals. In addition, elevated counts of human CD3 positive (hCD3$^+$) T cells were measured in both compartments upon treatment ($p < 0.0001$ for blood, $p = 0.005$ for bone marrow for ppp-RNA treated vs. untreated animals), suggesting enhanced immune cell expansion after ppp-RNA therapy.

---

[13] Results as described in Ruzicka, Koenig et al. 2020 with some modifications
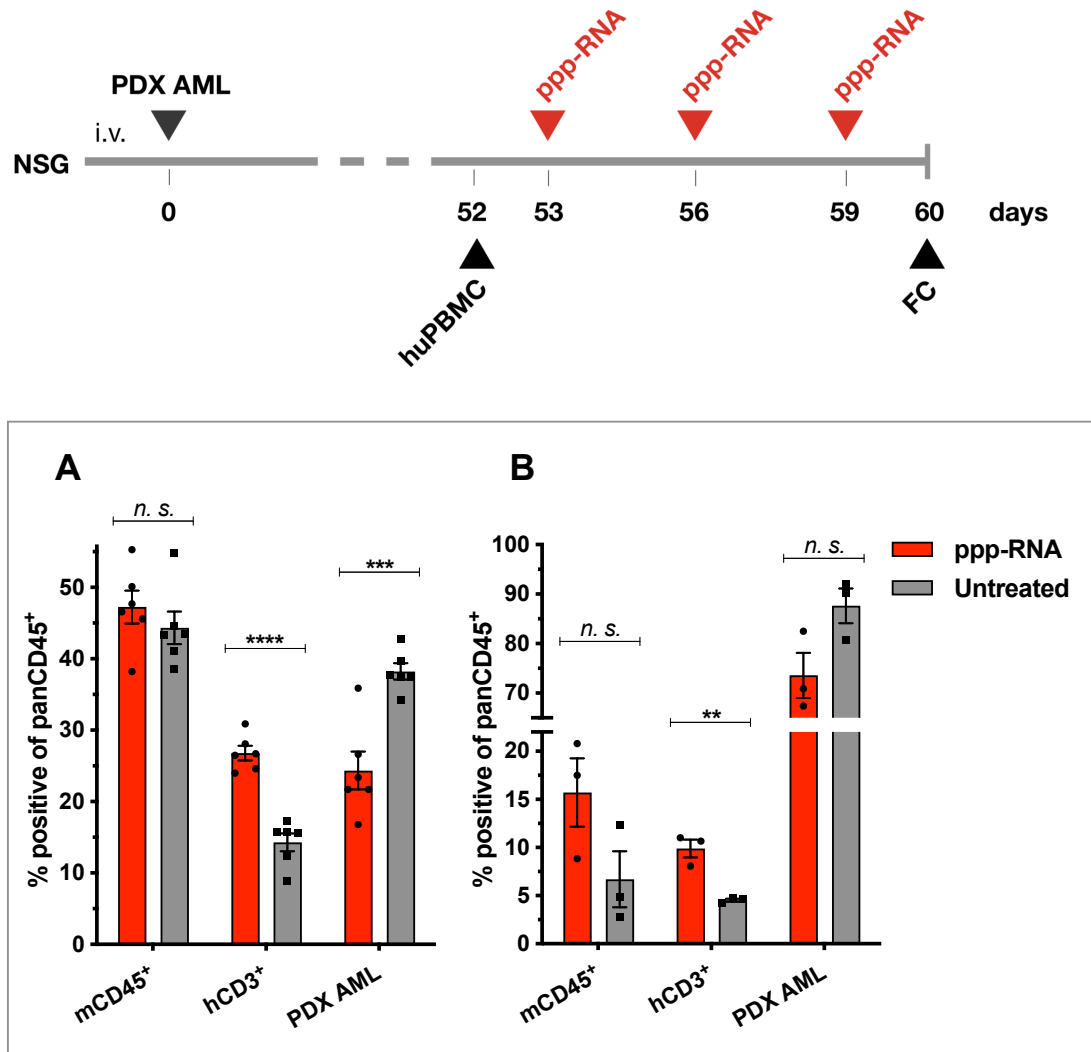
Figure 15. Efficacy of ppp-RNA in a humanized mouse model of AML. 12 NSG mice were inoculated with 4.5×10^5 PDX AML 491 cells i.v. on day 0 and 10^7 human PBMCs were injected on day 52. ppp-RNA treatment (n = 6) was given on days 53, 56 and 59. Mice were sacrificed 12 hours after the last treatment on day 60. Single cell suspensions of peripheral blood (A) and bone marrow (B) were analyzed by flow cytometry (FC), determining levels of mCD45+ and hCD3+ relating to panCD45+ cells. Tumor burden was determined by detection of mCherry positive cells. Bar charts depict mean values with SEM. Statistical significance was determined using Student's t-test with comparisons indicated by brackets. Figure and figure legend modified from Ruzicka, Koenig et al. 2020.

4. Discussion

4.1 ppp-RNA therapy can lead to full AML remission in mice

AML is a malignant hematologic disease that has remained challenging to treat ever since it had first been described. While chemotherapy and SCT may achieve full remission in a fraction of patients, the prognosis of the disease up to date is poor, making alternative treatment strategies urgently needed. In this work I investigated the therapeutic potential of systemic ppp-RNA immunotherapy, which allows to mimic a viral infection via the innate immune receptor RIG-I and thus points an immune response against antigens present in tumor cells. In various preclinical studies, this approach has been explored and led to promising results in the treatment of multiple solid malignancies (Poeck et al. 2008, Besch et al. 2009, Tormo et al. 2009, Yuan et al. 2015, Elion et al. 2018). In contrast, no studies report on ppp-RNA treatment in hematologic malignancies. I identified a mechanism in AML-bearing mice that led to immune cell-mediated rejection of tumor cells, establishing complete remission and an immunological memory in a fraction of animals.

4.1.1 Manual tumor inoculation and the xenoantigen GFP as possible sources of bias

To rule out potential bias such as uneven tumor growth between animals or failing tumor engraftment due to minor variations in the number of injected tumor cells, I inoculated WT mice with differing numbers of C1498/GFP AML cells. The survival of the mice was consistent even when using a quarter dose of tumor cells for inoculation, thus making the mode of manual injections for AML induction an unlikely source of error. Further, I decided to investigate whether tumor rejection in this model was AML specific or caused by the xenoantigen GFP. It has recently been shown that GFP expression enhances the immunogenicity of cells and diminishes their lifetime (Ansari et al. 2016). Another study demonstrated that the expression of GFP in bone marrow cells itself is sufficient to lead to their complete

rejection over time if transplanted into immunocompetent recipient mice, while in contrast, GFP negative cells withstood rejection (Bubnic et al. 2005). This raised the question as to whether the effect of ppp-RNA in my model of AML would remain consistent if cells did not express GFP. The survival data raised in C1498 WT AML inoculated mice demonstrate that the effect of the treatment is not limited to GFP-expressing cells. However, only a repetition of the experiment with increased numbers of mice could give a definite answer on how strongly long-term survival depends on the expression of GFP in the tumor cells. Further, rechallenging ppp-RNA treated, C1498/GFP AML surviving mice with C1498 WT AML cells could provide us with information on how relevant the xenoantigen is in immediate and in memory immune responses. Unfortunately, this approach was not feasible due to limited numbers of surviving mice which were prioritized for different objectives.

4.1.2 Non-responsiveness to immunotherapy

Most immunotherapeutic approaches show a characteristic portion of non-responsive tumor patients, and the underlying causes mostly remain elusive to the scientific community up to date. ppp-RNA treatment poses no exception: While most mice benefitted from the treatment with regard to survival, full remission was only achieved in about 19% of the animals. The comparability of my mouse model with real world patient data is of course limited, as I used an inbred mouse strain offering much less genetic diversity than it is the case in patient populations. Nevertheless, the parallels are worth noting. My observations regarding the fraction of survivors are in accord with studies evaluating the therapeutic potential of ppp-RNA in other tumor entities such as pancreatic cancer, where remission rates of around 6% were achieved with plain ppp-RNA and 20% with bifunctional ppp-RNA treatment (Ellermeier et al. 2013), the latter of which combines RIG-I stimulation with silencing of tumor driving genes by RNA interference.

In order to better understand the partial responsiveness to this treatment, I investigated the mechanisms involved in ppp-RNA-mediated rejection of AML cells in mice and explored immune evasive strategies of the disease to identify new points of action that could enhance treatment outcome.

4.2 Rejection of leukemic cells is mediated by immune cells

4.2.1 The role of RIG-I mediated apoptosis in the treatment of AML[14]

Two mechanisms of ppp-RNA-mediated tumor rejection have been previously described: A direct proapoptotic effect on the tumor cell independent of IFN (Besch et al. 2009, Tormo et al. 2009, Duewell et al. 2014) and a systemic, cell-mediated adaptive immune response. While previously a RIG-I dependent, direct cytotoxic effect of ppp-RNA on metastasized human melanoma cells in immunodeficient NSG mice has been described (Besch et al. 2009), my data show the complete absence of treatment benefits in C1498/GFP AML-bearing NSG mice, suggesting that in my model of AML, ppp-RNA treatment does not promote direct cytotoxicity or cytostasis. This is well explained by the fact that the C1498 AML cell line resists transfection with most commercially available RNA transfection reagents *in vitro* and with all tested by our group *in vivo*, indicating that the absence of direct cytotoxicity *in vivo* may be based on suboptimal means of drug delivery and poor transfectability rather than dysfunctional RIG-I signaling in the tumor cells.

4.2.2 CD8^{+} and CD4^{+} T cells mediate ppp-RNA induced rejection of AML cells[14]

The rejection of leukemic cells in my model of AML appeared to depend on the presence of cellular immunity. RIG-I activation is known to result in cytokine release, linking the innate immune response to the adaptive immune system via enhanced antigen-presentation on tumor cells and APCs as well as activation of

---

[14] With some modifications as described in Ruzicka, Koenig et al. 2020

adaptive immune cells (Hochheiser et al. 2016). Using depleting antibodies directed against different immune cell subsets in C1498/GFP AML-bearing WT mice, I identified CD4+ and CD8+ T cells as mediators of the treatment response, while B and NK cells appeared dispensable. These findings are in contrast to studies identifying NK cells as mediators of ppp-RNA induced anti-tumor responses against B16 melanoma cells (Poeck et al. 2008). However, in models of pancreatic cancer (Ellermeier et al. 2013) and hepatocellular carcinoma (unpublished data), NK cell depletion also failed to affect treatment outcomes negatively, suggesting that the underlying mechanisms of ppp-RNA therapy greatly vary depending on the tumor entity.

4.3 Intact RIG-I and IFNAR signaling are crucial for treatment outcome[15]

4.3.1 RIG-I and the possible involvement of TLRs in ppp-RNA therapy

MAVS is an adaptor protein essential for RIG-I downstream signaling. As *Rig-I-/-* mice on C57BL/6 background are not viable, I used *Mavs-/-* mice to evaluate the role of RIG-I and the possible contribution of off-target effects on the outcome of ppp-RNA treatment. Intact RIG-I signaling via MAVS in the host turned out to be of central importance for ppp-RNA treatment outcome, especially with regard to long-term survival, as the overall survival of *Mavs-/-* mice was inferior to the survival of WT mice. Of note, long-term survival and formation of an immunological memory was observed in WT mice exclusively. This indicates that intact RIG-I signaling is essential to achieve long-term remission, which is likely explained by the enhanced proinflammatory environment mediated by cytokine and particularly interferon release following its activation, eventually leading to augmented antigen cross-presentation via APCs and immune cell recruitment.

The residual effects of ppp-RNA treatment in *Mavs-/-* mice may be accounted for by the involvement of TLR7, an innate immune receptor with the ability to sense viral dsRNA and thus ppp-RNA, too (Hornung et al. 2005). Previous studies show

---

[15] With some modifications as described in Ruzicka, Koenig et al. 2020

that repeated activation of TLR7 in mice led to downregulation of the receptor (Bourquin et al. 2011). This could explain why in *Mavs*$^{-/-}$ mice, CXCL10 induction diminished over time as ppp-RNA therapy was given repeatedly, while chemokine levels in WT mice remained constant (Figure 7). Despite the likely activation of TLR7 by ppp-RNA treatment, the therapeutic outcome has previously been shown to remain unimpaired in *Tlr7*$^{-/-}$ mice (Poeck et al. 2008, Ellermeier et al. 2013), again underlining that independently of off-target involvement, RIG-I or MAVS, respectively, are the critical target receptors for ppp-RNA therapy.

4.3.2 ppp-RNA triggers IFN release in a model of disseminated AML

Type I IFN plays a critical role when it comes to the induction of anti-tumoral immune responses by activating immune cells and enhancing antigen presentation. Consistently with previously published results (Poeck et al. 2008), intact IFNAR signaling in the host proved to be a key factor for ppp-RNA treatment efficacy in my model of AML. Disseminated leukemia is known for its inability to induce type I IFN in contrast to subcutaneously grown leukemic tumors, thus failing to activate cellular anti-tumor immunity (Curran et al. 2016). Elevated levels of CXCL10 after treatment suggest that ppp-RNA therapy does induce IFN in my model of disseminated AML, and thus paves the way for a cellular immune response as described in 4.2. Interestingly, the treatment of AML-bearing mice with IFN only did not result in any notable effect, suggesting that the effects of ppp-RNA therapy are mediated by, but not limited to effects of type I IFN release. The precise mode of action of the treatment appears to go beyond IFN release and may be subject to future studies.

4.4 ppp-RNA may reduce the risk of relapsing AML[16]

4.4.1 Curative ppp-RNA treatment induces an immunological memory protective of relapses

The treatment of AML is challenging particularly due to the fact that patients remain prone to relapses even after initial complete remission. Taking the observation into account that ppp-RNA therapy induces the formation of an immunological long-term memory, this treatment appears particularly interesting in the context of AML as it holds the potential to establish vaccination-like immunity and thus prevent such relapses. I discovered that all ppp-RNA treated mice surviving C1498/GFP AML formed an immunological memory protective of rechallenges with C1498/GFP AML cells.

The formation of an immunological memory after curative immunotherapy is not uncommon in treatments based on adaptive immune responses. Previous studies compared memory responses upon tumor rechallenge in mice that have been cured of solid tumors by either viral oncolytic immunotherapy (VOI) or chemotherapy. Interestingly, 93-100% of VOI treated, tumor-surviving mice withstood the rechallenge while only 0-20% of chemotherapy treated animals did (Gao et al. 2018). Taken together with my data, it seems that the pursuit of immune-based, memory inducing treatment strategies for AML as opposed to well established chemotherapeutic approaches holds the potential to minimize the risk of relapses, which yet remain the clinically most challenging feature of the disease.

4.4.2 Memory responses are mediated by CD8+ T cells

By adoptively transferring CD8+ T cells from AML surviving mice into AML-bearing WT mice I learned that the memory responses are mediated by cytotoxic T cells. The transfer prolonged survival significantly, yet failed to establish long-term remission, likely because the transferred T cells were not activated or

---

[16] With some modifications as described in Ruzicka, Koenig et al. 2020

expanded with regard to antigen-specificity *ex vivo*. Therefore, it is fair to assume that the transfer only contained a small fraction of AML specific T cells. Together with the lack of cognate APCs and T helper cells, this explains why the *in vivo* expansion of the transferred cells remained insufficient to establish a long-lasting remission. A co-transfer of CD4^{+} T cells from AML surviving mice and significantly higher numbers of transferred T cells (as laid out by Gao and Bergman 2018) may have helped to achieve higher remission rates, but were technically not feasible.

4.5 ppp-RNA primes AML cells for checkpoint inhibition therapy[17]

My studies revealed the central role IFN release plays in the treatment of AML with ppp-RNA. IFN is known to upregulate PD-L1 expression on tumor cells, thus limiting cellular immune responses (Freeman et al. 2000). *In vitro* and *in vivo*, I found that C1498/GFP AML cells pose no exception to this phenomenon, leading to the hypothesis that the treatment could benefit from simultaneous checkpoint inhibition therapy.

The data show that antibody-mediated blockade of PD-1 augmented the therapeutic efficacy of ppp-RNA while monotherapy with the antibody remained without any effect, suggesting a priming role of ppp-RNA for the antibody to become therapeutically relevant. These findings are in conflict with previous studies showing partial efficacy of anti-PD-L1 monotherapy in the C1498/GFP AML model (Zhang et al. 2009). The difference in findings, however, may be explained by the fact that the authors used double the dose of inhibitory antibody which additionally was targeted against PD-L1, not PD-1. Preliminary data from a single experiment of mine indicate that the synergistic nature of ppp-RNA and an anti-PD-1 antibody may hold the potential for even higher survival rates if the dose of ppp-RNA is escalated.

---

[17] With some modifications as described in Ruzicka, Koenig et al. 2020

The concept of a priming agent sensitizing leukemic cells to checkpoint inhibition has previously been investigated in the context of oncolytic viruses (Shen et al. 2016) and has recently been considered for agonists of stimulator of interferon genes (STING) (Curran et al. 2016). Together with these findings, my data underline the potential of targeting innate PRRs to trigger IFN-mediated immune responses while simultaneously blocking IFN-regulated immune checkpoints, and encourages to explore further immune checkpoints as potential targets to optimize treatment outcomes. The priming character of ppp-RNA on checkpoint inhibition therapy in this particular model of AML may be of high clinical relevance as critical fractions of AML patients remain non-responsive to (mono-)therapy with checkpoint inhibitors (Bruserud et al. 2019, Daver et al. 2019, Stahl et al. 2019).

4.6 Replicability in humanized mice demonstrates potential for clinical translation[18]

To evaluate its potential for clinical translation, I designed a humanized mouse model that would allow me to investigate the effects of ppp-RNA immunotherapy on patient-derived AML cells in a setting based on the idea of allogeneic donor lymphocyte infusion (DLI). DLI is a treatment that was initially established for patients suffering from relapsed chronic myeloid leukemia after SCT. Patients receive lymphocytes of their respective stem cell donor after SCT in order to enhance the graft-versus-leukemia (GvL) effect, which can obviate the need of a second SCT. Based on recent findings, DLI may be beneficial in the case of relapsed high-risk AML after SCT (Schmid et al. 2007, Schmid et al. 2018) or as a preventive measure after SCT (Takami et al. 2014).

To simulate a comparable setting, I infused human PDX AML-bearing NSG mice with allogeneic human PBMCs. The infusion of PBMCs resulted in donor dependent graft-versus-host (GvH) reactions of varying intensity, in certain cases pronounced enough for the experiment to be terminated before reaching a

---

[18] With some modifications as described in Ruzicka, Koenig et al. 2020

relevant end point. The slow growth of PDX AML cells and looming GvH reactions forced the PBMC infusion to be carried out at late, close to terminal stages of disease using low numbers of transfused PBMCs. This left me a window of only a few days to conduct treatment and analyses.

Nevertheless, I observed a reduction of tumor mass in the peripheral blood and bone marrow of ppp-RNA treated mice, while at the same time CD3$^+$ T cell counts rose in the respective tissues, indicating a boosted GvL reaction triggered by ppp-RNA. Importantly, no signs of accelerated GvHD were observed in ppp-RNA-treated mice within the short time frame I monitored them after ppp-RNA treatment. More detailed studies will be needed to fully evaluate whether ppp-RNA treatment can potentiate the effects of DLI in relapsed AML patients after SCT. It also remains unclear whether the anti-leukemic effect is mediated by direct proapoptotic effects of ppp-RNA on the tumor cells or via T cell induced cytotoxicity. Lastly, the use of HLA-matched PDX AML cells and PBMCs would allow to investigate how much of the effect relies on AML specificity of the transfused leukocytes rather than the HLA-mismatch itself.

5. Summary

AML is a clonal disease of hematopoietic precursor cells with a poor prognosis. While immunotherapeutic approaches for hematologic malignancies are on the rise, remission rates in AML remain low, making new treatment strategies urgently needed. I decided to investigate the potential of RIG-I-targeted immunotherapy using ppp-RNA in the treatment of AML, which allows to induce an immunological anti-tumor response by mimicking a viral infection. RIG-I is a cytoplasmic innate immune receptor that senses viral RNA, upon which it triggers the release of type I IFNs and proinflammatory cytokines, thus inducing an adaptive cellular immune response (Ruzicka et al. 2020).

The treatment significantly prolonged the survival of C1498/GFP AML-bearing C57BL/6 mice and established complete remission and immunological memory formation in a fraction of almost 20% of the animals. The outcome was strongly dependent on the presence of cellular immunity, particularly CD4$^+$ and CD8$^+$ T cells, while NK and B cells appeared dispensable. The response further depended on intact IFNAR and MAVS expression in the host, indicating that in this model systemic, proinflammatory effects and immune cell activation are the central mechanisms of AML rejection. Further, I observed upregulated PD-L1 expression on AML cells after treatment and hence a possibility to sensitize these cells to therapeutic anti-PD-1 checkpoint inhibition *in vivo*. Lastly, I demonstrated anti-leukemic effects of ppp-RNA therapy in immune-reconstituted humanized mice bearing patient-derived, disseminated AML. Beyond reduction of patient-derived tumor cells, I observed enhanced fractions of human CD3$^+$ T cells in both blood and bone marrow after the treatment.

Particularly due to its ability to establish a state of complete remission while forming an immunological memory, my findings show that ppp-RNA therapy is a promising strategy for the treatment of AML.

6. Zusammenfassung

AML ist eine klonale Erkrankung hämatopoetischer Vorläuferzellen und mit einer schlechten Prognose verknüpft. Trotz der zunehmenden Bedeutung immuntherapeutischer Ansätze in der Behandlung hämatologischer Neoplasien bleiben die Remissionsraten von AML-Patienten unzureichend und verdeutlichen den Bedarf neuer Behandlungsstrategien. Im Rahmen der vorliegenden Arbeit entschied ich mich, das Potential von ppp-RNA und somit RIG-I-vermittelter Immuntherapie für die Behandlung der AML zu untersuchen. Dieser Ansatz erlaubt es, eine systemische Immunantwort gegen Tumoren mittels viraler Mimikry zu induzieren. RIG-I ist ein zytoplasmatischer Rezeptor des angeborenen Immunsystems mit der Eigenschaft, virale RNA zu erkennen und über die Induktion proinflammatorischer Zytokine und IFN eine Antwort des erworbenen Immunsystems einzuleiten.

Die Therapie führte zu einer signifikanten Überlebenszeitverlängerung von C57BL/6 Mäusen mit C1498/GFP AML und kompletter Remission einschließlich der Bildung eines immunologischen Gedächtnisses in fast 20% der Versuchstiere. Der Therapieerfolg hing maßgeblich vom Vorhandensein CD4+ und CD8+ T-Lymphozyten ab, wohingegen NK- und B-Zellen von untergeordneter Bedeutung zu sein schienen. Die Abhängigkeit des Therapieerfolges von intakter IFNAR- und MAVS-Expression im murinen Organismus verdeutlicht, dass systemische, proinflammatorische Effekte und Immunzellaktivierung im Vordergrund des Therapiemechanismus stehen. Interessanterweise zeigte sich, dass die Therapie mit ppp-RNA die Expression von PD-L1 auf AML Zellen induzierte und eine Sensitivität dieser Zellen gegenüber therapeutischer anti-PD-1 Checkpoint-Blockade *in vivo* hervorrief. Darüber hinaus führte die Behandlung zu einer Verringerung der Last patientenstämmiger AML Zellen in immunrekonstituierten, humanisierten Mäusen bei gleichzeitig erhöhter Infiltration tumorbefallenen Gewebes durch CD3+ T-Lymphozyten.

Zusammenfassend lässt sich sagen, dass ppp-RNA in der Therapie der AML nicht nur das Potential für eine komplette onkologische Remission birgt, sondern darüber hinaus auch eine Immunisierung gegen die Erkrankung induzieren und ihr somit eine rezidivprophylaktische Wirkung zugeschrieben werden kann.

7. Bibliography

Ansari, A. M., A. K. Ahmed, A. E. Matsangos, F. Lay, L. J. Born, G. Marti, J. W. Harmon and Z. Sun. Cellular GFP Toxicity and Immunogenicity: Potential Confounders in in Vivo Cell Tracking Experiments. *Stem Cell Rev* 2016; 12.5: 553-559.

Ascierto, P. A., G. V. Long, C. Robert, B. Brady, C. Dutriaux, A. M. Di Giacomo, L. Mortier, J. C. Hassel, P. Rutkowski, C. McNeil, E. Kalinka-Warzocha, K. J. Savage, M. M. Hernberg, C. Lebbe, J. Charles, C. Mihalcioiu, V. Chiarion-Sileni, C. Mauch, F. Cognetti, L. Ny, A. Arance, I. M. Svane, D. Schadendorf, H. Gogas, A. Saci, J. Jiang, J. Rizzo and V. Atkinson. Survival Outcomes in Patients With Previously Untreated BRAF Wild-Type Advanced Melanoma Treated With Nivolumab Therapy: Three-Year Follow-up of a Randomized Phase 3 Trial. *JAMA Oncol* 2018.

Bald, T., J. Landsberg, D. Lopez-Ramos, M. Renn, N. Glodde, P. Jansen, E. Gaffal, J. Steitz, R. Tolba, U. Kalinke, A. Limmer, G. Jonsson, M. Holzel and T. Tuting. Immune cell-poor melanomas benefit from PD-1 blockade after targeted type I IFN activation. *Cancer Discov* 2014; 4.6: 674-687.

Bardhan, K., T. Anagnostou and V. A. Boussiotis. The PD1:PD-L1/2 Pathway from Discovery to Clinical Implementation. *Front Immunol* 2016; 7.550.

Besch, R., H. Poeck, T. Hohenauer, D. Senft, G. Hacker, C. Berking, V. Hornung, S. Endres, T. Ruzicka, S. Rothenfusser and G. Hartmann. Proapoptotic signaling induced by RIG-I and MDA-5 results in type I interferon-independent apoptosis in human melanoma cells. *J Clin Invest* 2009; 119.8: 2399-2411.

Blasius, A. L. and B. Beutler. Intracellular toll-like receptors. *Immunity* 2010; 32.3: 305-315.

Bourquin, C., C. Hotz, D. Noerenberg, A. Voelkl, S. Heidegger, L. C. Roetzer, B. Storch, N. Sandholzer, C. Wurzenberger, D. Anz and S. Endres. Systemic cancer therapy with a small molecule agonist of toll-like receptor 7 can be improved by circumventing TLR tolerance. *Cancer Res* 2011; 71.15: 5123-5133.

Brubaker, S. W., K. S. Bonham, I. Zanoni and J. C. Kagan. Innate immune pattern recognition: a cell biological perspective. *Annu Rev Immunol* 2015; 33.257-290.

Bruserud, O. and E. Leufven. Immunosuppression And Immunotargeted Therapy In Acute Myeloid Leukemia - The Potential Use Of Checkpoint Inhibitors In Combination With Other Treatments. *Curr Med Chem* 2019.

Bubnic, S. J., A. Nagy and A. Keating. Donor hematopoietic cells from transgenic mice that express GFP are immunogenic in immunocompetent recipients. *Hematology* 2005; 10.4: 289-295.

Chow, K. T., M. Gale, Jr. and Y. M. Loo. RIG-I and Other RNA Sensors in Antiviral Immunity. *Annu Rev Immunol* 2018; 36.667-694.

Curran, E., X. Chen, L. Corrales, D. E. Kline, T. W. Dubensky, Jr., P. Duttagupta, M. Kortylewski and J. Kline. STING Pathway Activation Stimulates Potent Immunity against Acute Myeloid Leukemia. *Cell Rep* 2016; 15.11: 2357-2366.

Daver, N., G. Garcia-Manero, S. Basu, P. C. Boddu, M. Alfayez, J. E. Cortes, M. Konopleva, F. Ravandi-Kashani, E. Jabbour, T. Kadia, G. M. Nogueras-Gonzalez, J. Ning, N. Pemmaraju, C. D. DiNardo, M. Andreeff, S. A. Pierce, T. Gordon, S. M. Kornblau, W. Flores, Z. Alhamal, C. Bueso-Ramos, J. L. Jorgensen, K. P. Patel, J. Blando, J. P. Allison, P. Sharma and H. Kantarjian. Efficacy, Safety, and Biomarkers of Response to Azacitidine and Nivolumab in Relapsed/Refractory Acute Myeloid Leukemia: A Nonrandomized, Open-Label, Phase II Study. *Cancer Discov* 2019; 9.3: 370-383.

Dohner, H., E. H. Estey, S. Amadori, F. R. Appelbaum, T. Buchner, A. K. Burnett, H. Dombret, P. Fenaux, D. Grimwade, R. A. Larson, F. Lo-Coco, T. Naoe, D. Niederwieser, G. J. Ossenkoppele, M. A. Sanz, J. Sierra, M. S. Tallman, B. Lowenberg, C. D. Bloomfield and L. European. Diagnosis and management of acute myeloid leukemia in adults: recommendations from an international expert panel, on behalf of the European LeukemiaNet. *Blood* 2010; 115.3: 453-474.

Dohner, H., D. J. Weisdorf and C. D. Bloomfield. Acute Myeloid Leukemia. *N Engl J Med* 2015; 373.12: 1136-1152.

Dores, G. M., S. S. Devesa, R. E. Curtis, M. S. Linet and L. M. Morton. Acute leukemia incidence and patient survival among children and adults in the United States, 2001-2007. *Blood* 2012; 119.1: 34-43.

Duewell, P., A. Steger, H. Lohr, H. Bourhis, H. Hoelz, S. V. Kirchleitner, M. R. Stieg, S. Grassmann, S. Kobold, J. T. Siveke, S. Endres and M. Schnurr. RIG-I-like helicases induce immunogenic cell death of pancreatic cancer cells and sensitize tumors toward killing by CD8(+) T cells. *Cell Death Differ* 2014; 21.12: 1825-1837.

Eisfeld, A. K., J. Kohlschmidt, K. Mrozek, J. S. Blachly, C. J. Walker, D. Nicolet, S. Orwick, S. E. Maharry, A. J. Carroll, R. M. Stone, A. de la Chapelle, E. S. Wang, J. E. Kolitz, B. L. Powell, J. C. Byrd and C. D. Bloomfield. Mutation patterns identify adult patients with de novo acute myeloid leukemia aged 60 years or older who respond favorably to standard chemotherapy: an analysis of Alliance studies. *Leukemia* 2018.

Elion, D. L., M. E. Jacobson, D. J. Hicks, B. Rahman, V. Sanchez, P. I. Gonzales-Ericsson, O. Fedorova, A. M. Pyle, J. T. Wilson and R. S. Cook. Therapeutically Active RIG-I Agonist Induces Immunogenic Tumor Cell Killing in Breast Cancers. *Cancer Res* 2018; 78.21: 6183-6195.

Ellermeier, J., J. Wei, P. Duewell, S. Hoves, M. R. Stieg, T. Adunka, D. Noerenberg, H. J. Anders, D. Mayr, H. Poeck, G. Hartmann, S. Endres and M. Schnurr. Therapeutic efficacy of bifunctional siRNA combining TGF-beta1 silencing with RIG-I activation in pancreatic cancer. *Cancer Res* 2013; 73.6: 1709-1720.

Freeman, G. J., A. J. Long, Y. Iwai, K. Bourque, T. Chernova, H. Nishimura, L. J. Fitz, N. Malenkovich, T. Okazaki, M. C. Byrne, H. F. Horton, L. Fouser, L. Carter, V. Ling, M. R. Bowman, B. M. Carreno, M. Collins, C. R. Wood and T. Honjo. Engagement of the PD-1 immunoinhibitory receptor by a novel B7 family member leads to negative regulation of lymphocyte activation. *J Exp Med* 2000; 192.7: 1027-1034.

Gao, Y. and I. Bergman. Potent Antitumor T-Cell Memory Is Generated by Curative Viral Oncolytic Immunotherapy But Not Curative Chemotherapy. *Anticancer Res* 2018; 38.12: 6621-6629.

Gubin, M. M., X. Zhang, H. Schuster, E. Caron, J. P. Ward, T. Noguchi, Y. Ivanova, J. Hundal, C. D. Arthur, W. J. Krebber, G. E. Mulder, M. Toebes, M. D. Vesely, S. S. Lam, A. J. Korman, J. P. Allison, G. J. Freeman, A. H. Sharpe, E. L. Pearce, T. N. Schumacher, R. Aebersold, H. G. Rammensee, C. J. Melief, E. R. Mardis, W. E. Gillanders, M. N. Artyomov and R. D. Schreiber. Checkpoint blockade cancer immunotherapy targets tumour-specific mutant antigens. *Nature* 2014; 515.7528: 577-581.

Hemann, E. A., M. Gale, Jr. and R. Savan. Interferon Lambda Genetics and Biology in Regulation of Viral Control. *Front Immunol* 2017; 8.1707.

Hochheiser, K., M. Klein, C. Gottschalk, F. Hoss, S. Scheu, C. Coch, G. Hartmann and C. Kurts. Cutting Edge: The RIG-I Ligand 3pRNA Potently Improves CTL Cross-Priming and Facilitates Antiviral Vaccination. *J Immunol* 2016; 196.6: 2439-2443.

Hoffmann, H. H., W. M. Schneider and C. M. Rice. Interferons and viruses: an evolutionary arms race of molecular interactions. *Trends Immunol* 2015; 36.3: 124-138.

Hornung, V., M. Guenthner-Biller, C. Bourquin, A. Ablasser, M. Schlee, S. Uematsu, A. Noronha, M. Manoharan, S. Akira, A. de Fougerolles, S. Endres and G. Hartmann. Sequence-specific potent induction of IFN-alpha by short interfering RNA in plasmacytoid dendritic cells through TLR7. *Nat Med* 2005; 11.3: 263-270.

Hornung, V., J. Ellegast, S. Kim, K. Brzozka, A. Jung, H. Kato, H. Poeck, S. Akira, K. K. Conzelmann, M. Schlee, S. Endres and G. Hartmann. 5'-Triphosphate RNA is the ligand for RIG-I. *Science* 2006; 314.5801: 994-997.

Ishida, Y., Y. Agata, K. Shibahara and T. Honjo. Induced expression of PD-1, a novel member of the immunoglobulin gene superfamily, upon programmed cell death. *EMBO J* 1992; 11.11: 3887-3895.

Janeway, C. A., Jr. Approaching the asymptote? Evolution and revolution in immunology. *Cold Spring Harb Symp Quant Biol* 1989; 54 Pt 1.1-13.

Janeway, C. A., Jr., P. Travers, M. Walport and M. Shlomchik (2001). Immunobiology: The Immune System in Health and Disease. 5th Edition. New York, Garland Science.

Janeway, C. A., Jr. and R. Medzhitov. Innate immune recognition. *Annu Rev Immunol* 2002; 20.197-216.

Kawasaki, T. and T. Kawai. Toll-like receptor signaling pathways. *Front Immunol* 2014; 5.461.

Kell, A. M. and M. Gale, Jr. RIG-I in RNA virus recognition. *Virology* 2015; 479-480.110-121.

Lichtenegger, F. S., C. Krupka, S. Haubner, T. Kohnke and M. Subklewe. Recent developments in immunotherapy of acute myeloid leukemia. *J Hematol Oncol* 2017; 10.1: 142.

Link, D. C., G. Kunter, Y. Kasai, Y. Zhao, T. Miner, M. D. McLellan, R. E. Ries, D. Kapur, R. Nagarajan, D. C. Dale, A. A. Bolyard, L. A. Boxer, K. Welte, C. Zeidler, J. Donadieu, C. Bellanne-Chantelot, J. W. Vardiman, M. A. Caligiuri, C. D. Bloomfield, J. F. DiPersio, M. H. Tomasson, T. A. Graubert, P. Westervelt, M. Watson, W. Shannon, J. Baty, E. R. Mardis, R. K. Wilson and T. J. Ley. Distinct patterns of mutations occurring in de novo AML versus AML arising in the setting of severe congenital neutropenia. *Blood* 2007; 110.5: 1648-1655.

Livak, F., D. B. Burtrum, L. Rowen, D. G. Schatz and H. T. Petrie. Genetic modulation of T cell receptor gene segment usage during somatic recombination. *J Exp Med* 2000; 192.8: 1191-1196.

Ma, F., B. Li, Y. Yu, S. S. Iyer, M. Sun and G. Cheng. Positive feedback regulation of type I interferon by the interferon-stimulated gene STING. *EMBO Rep* 2015; 16.2: 202-212.

Major, J., S. Crotta, M. Llorian, T. M. McCabe, H. H. Gad, S. L. Priestnall, R. Hartmann and A. Wack. Type I and III interferons disrupt lung epithelial repair during recovery from viral infection. *Science* 2020; 369.6504: 712-717.

Mogensen, T. H. Pathogen recognition and inflammatory signaling in innate immune defenses. *Clin Microbiol Rev* 2009; 22.2: 240-273, Table of Contents.

Mopin, A., V. Driss and C. Brinster. A Detailed Protocol for Characterizing the Murine C1498 Cell Line and its Associated Leukemia Mouse Model. *J Vis Exp* 2016;116.

Obst, R. The Timing of T Cell Priming and Cycling. *Front Immunol* 2015; 6.563.

Onoguchi, K., M. Yoneyama and T. Fujita. Retinoic acid-inducible gene-I-like receptors. *J Interferon Cytokine Res* 2011; 31.1: 27-31.

Pascutti, M. F., S. Geerman, N. Collins, G. Brasser, B. Nota, R. Stark, F. Behr, A. Oja, E. Slot, E. Panagioti, J. E. Prier, S. Hickson, M. C. Wolkers, M. H. M. Heemskerk, P. Hombrink, R. Arens, L. K. Mackay, K. van Gisbergen and M. A. Nolte. Peripheral and systemic antigens elicit an expandable pool of resident memory CD8(+) T cells in the bone marrow. *Eur J Immunol* 2019.

Poeck, H., R. Besch, C. Maihoefer, M. Renn, D. Tormo, S. S. Morskaya, S. Kirschnek, E. Gaffal, J. Landsberg, J. Hellmuth, A. Schmidt, D. Anz, M. Bscheider, T. Schwerd, C. Berking, C. Bourquin, U. Kalinke, E. Kremmer, H. Kato, S. Akira, R. Meyers, G. Hacker, M. Neuenhahn, D. Busch, J. Ruland, S. Rothenfusser, M. Prinz, V. Hornung, S. Endres, T. Tuting and G. Hartmann. 5'-Triphosphate-siRNA: turning gene silencing and Rig-I activation against melanoma. *Nat Med* 2008; 14.11: 1256-1263.

Robert, C., G. V. Long, B. Brady, C. Dutriaux, M. Maio, L. Mortier, J. C. Hassel, P. Rutkowski, C. McNeil, E. Kalinka-Warzocha, K. J. Savage, M. M. Hernberg, C. Lebbe, J. Charles, C. Mihalcioiu, V. Chiarion-Sileni, C. Mauch, F. Cognetti, A. Arance, H. Schmidt, D. Schadendorf, H. Gogas, L. Lundgren-Eriksson, C. Horak, B. Sharkey, I. M. Waxman, V. Atkinson and P. A. Ascierto. Nivolumab in previously untreated melanoma without BRAF mutation. *N Engl J Med* 2015; 372.4: 320-330.

Ruzicka, M., L. M. Koenig, S. Formisano, D. F. R. Boehmer, B. Vick, E. M. Heuer, H. Meinl, L. Kocheise, M. Zeitlhofler, J. Ahlfeld, S. Kobold, S. Endres, M. Subklewe, P. Duewell, M. Schnurr, I. Jeremias, F. S. Lichtenegger and S. Rothenfusser. RIG-I-based immunotherapy enhances survival in preclinical AML models and sensitizes AML cells to checkpoint blockade. *Leukemia* 2020; 34.4: 1017-1026.

Schlee, M., A. Roth, V. Hornung, C. A. Hagmann, V. Wimmenauer, W. Barchet, C. Coch, M. Janke, A. Mihailovic, G. Wardle, S. Juranek, H. Kato, T. Kawai, H. Poeck, K. A.

Fitzgerald, O. Takeuchi, S. Akira, T. Tuschl, E. Latz, J. Ludwig and G. Hartmann. Recognition of 5' triphosphate by RIG-I helicase requires short blunt double-stranded RNA as contained in panhandle of negative-strand virus. *Immunity* 2009; 31.1: 25-34.

Schlee, M. and G. Hartmann. Discriminating self from non-self in nucleic acid sensing. *Nat Rev Immunol* 2016; 16.9: 566-580.

Schmid, C., M. Labopin, A. Nagler, M. Bornhauser, J. Finke, A. Fassas, L. Volin, G. Gurman, J. Maertens, P. Bordigoni, E. Holler, G. Ehninger, E. Polge, N. C. Gorin, H. J. Kolb, V. Rocha and E. A. L. W. Party. Donor lymphocyte infusion in the treatment of first hematological relapse after allogeneic stem-cell transplantation in adults with acute myeloid leukemia: a retrospective risk factors analysis and comparison with other strategies by the EBMT Acute Leukemia Working Party. *J Clin Oncol* 2007; 25.31: 4938-4945.

Schmid, C., M. Labopin, N. Schaap, H. Veelken, M. Schleuning, M. Stadler, J. Finke, E. Hurst, F. Baron, O. Ringden, G. Bug, D. Blaise, J. Tischer, A. Bloor, J. Esteve, S. Giebel, B. Savani, N. C. Gorin, F. Ciceri, M. Mohty, A. Nagler and E. A. L. W. Party. Prophylactic donor lymphocyte infusion after allogeneic stem cell transplantation in acute leukaemia - a matched pair analysis by the Acute Leukaemia Working Party of EBMT. *Br J Haematol* 2018.

Shen, W., M. M. Patnaik, A. Ruiz, S. J. Russell and K. W. Peng. Immunovirotherapy with vesicular stomatitis virus and PD-L1 blockade enhances therapeutic outcome in murine acute myeloid leukemia. *Blood* 2016; 127.11: 1449-1458.

Stahl, M. and A. D. Goldberg. Immune Checkpoint Inhibitors in Acute Myeloid Leukemia: Novel Combinations and Therapeutic Targets. *Curr Oncol Rep* 2019; 21.4: 37.

Stanifer, M. L., K. Pervolaraki and S. Boulant. Differential Regulation of Type I and Type III Interferon Signaling. *Int J Mol Sci* 2019; 20.6.

Studeny, M., F. C. Marini, J. L. Dembinski, C. Zompetta, M. Cabreira-Hansen, B. N. Bekele, R. E. Champlin and M. Andreeff. Mesenchymal stem cells: potential precursors for tumor stroma and targeted-delivery vehicles for anticancer agents. *J Natl Cancer Inst* 2004; 96.21: 1593-1603.

Takami, A., S. Yano, H. Yokoyama, Y. Kuwatsuka, T. Yamaguchi, Y. Kanda, Y. Morishima, T. Fukuda, Y. Miyazaki, H. Nakamae, J. Tanaka, Y. Atsuta and H. Kanamori. Donor lymphocyte infusion for the treatment of relapsed acute myeloid leukemia after allogeneic hematopoietic stem cell transplantation: a retrospective analysis by the Adult Acute Myeloid Leukemia Working Group of the Japan Society for Hematopoietic Cell Transplantation. *Biol Blood Marrow Transplant* 2014; 20.11: 1785-1790.

Takaoka, A., S. Hayakawa, H. Yanai, D. Stoiber, H. Negishi, H. Kikuchi, S. Sasaki, K. Imai, T. Shibue, K. Honda and T. Taniguchi. Integration of interferon-alpha/beta signalling to p53 responses in tumour suppression and antiviral defence. *Nature* 2003; 424.6948: 516-523.

Tenen, D. G., R. Hromas, J. D. Licht and D. E. Zhang. Transcription factors, normal myeloid development, and leukemia. *Blood* 1997; 90.2: 489-519.

Tormo, D., A. Checinska, D. Alonso-Curbelo, E. Perez-Guijarro, E. Canon, E. Riveiro-Falkenbach, T. G. Calvo, L. Larribere, D. Megias, F. Mulero, M. A. Piris, R. Dash, P. M. Barral, J. L. Rodriguez-Peralto, P. Ortiz-Romero, T. Tuting, P. B. Fisher and M. S. Soengas. Targeted activation of innate immunity for therapeutic induction of autophagy and apoptosis in melanoma cells. *Cancer Cell* 2009; 16.2: 103-114.

Tumeh, P. C., C. L. Harview, J. H. Yearley, I. P. Shintaku, E. J. Taylor, L. Robert, B. Chmielowski, M. Spasic, G. Henry, V. Ciobanu, A. N. West, M. Carmona, C. Kivork, E. Seja, G. Cherry, A. J. Gutierrez, T. R. Grogan, C. Mateus, G. Tomasic, J. A. Glaspy, R. O. Emerson, H. Robins, R. H. Pierce, D. A. Elashoff, C. Robert and A. Ribas. PD-1 blockade induces responses by inhibiting adaptive immune resistance. *Nature* 2014; 515.7528: 568-571.

van Pesch, V., H. Lanaya, J. C. Renauld and T. Michiels. Characterization of the murine alpha interferon gene family. *J Virol* 2004; 78.15: 8219-8228.

Vick, B., M. Rothenberg, N. Sandhofer, M. Carlet, C. Finkenzeller, C. Krupka, M. Grunert, A. Trumpp, S. Corbacioglu, M. Ebinger, M. C. Andre, W. Hiddemann, S. Schneider, M. Subklewe, K. H. Metzeler, K. Spiekermann and I. Jeremias. An advanced preclinical mouse model for acute myeloid leukemia using patients' cells of various

genetic subgroups and in vivo bioluminescence imaging. *PLoS One* 2015; 10.3: e0120925.

Yoshimi, A., T. Toya, M. Kawazu, T. Ueno, A. Tsukamoto, H. Iizuka, M. Nakagawa, Y. Nannya, S. Arai, H. Harada, K. Usuki, Y. Hayashi, E. Ito, K. Kirito, H. Nakajima, M. Ichikawa, H. Mano and M. Kurokawa. Recurrent CDC25C mutations drive malignant transformation in FPD/AML. *Nat Commun* 2014; 5.4770.

Yuan, D., M. Xia, G. Meng, C. Xu, Y. Song and J. Wei. Anti-angiogenic efficacy of 5'-triphosphate siRNA combining VEGF silencing and RIG-I activation in NSCLCs. *Oncotarget* 2015; 6.30: 29664-29674.

Zhang, L., T. F. Gajewski and J. Kline. PD-1/PD-L1 interactions inhibit antitumor immune responses in a murine acute myeloid leukemia model. *Blood* 2009; 114.8: 1545-1552.

8. List of abbreviations

Abbreviation	Full term	First introduced (page no.)
5'	Five-prime	4
AB	Antibody	37
AML	Acute myeloid leukemia	1
APAF-1	Apoptotic protease-activating factor-1	5
APC	Antigen presenting cell	6
BCR	B cell receptor	6
BSA	Albumin Fraction V	13
C1498/GFP	Green fluorescent protein expressing C1498 AML cells	30
CAR	Chimeric antigen receptor	1
CARD	Caspase activation and recruitment domain	4
CD	Cluster of differentiation	4
CTLA-4	Cytotoxic T-lymphocyte-associated protein 4	8
CXCL10	C-X-C motif chemokine ligand 10	14
DC	Dendritic cell	2
DLI	Donor lymphocyte infusion	58
DMEM	Dulbecco's Modified Eagle's Medium	15
DMSO	Dimethyl sulfoxide	14
ds	Double-stranded	4
eGFP	Enhanced green fluorescent protein	19
ELISA	Enzyme-linked immunosorbent assay	22
FACS	Flow cytometry or fluorescence-activated cell sorting	22
FBS	Fetal bovine serum	15
FC	Flow cytometry	50
GFP	Green fluorescent protein	30

GvH	Graft-versus-host	58
GvHD	Graft-versus-host-disease	47
GvL	Graft-versus-leukemia	58
hCD3+	Human CD3 positive	49
hCD45+	Human CD45 positive	48
hp	Hairpin	25
HLA	Human Leukocyte Antigen	47
HPLC	High pressure liquid chromatography	24
i.p	Intraperitoneal(ly)	27
i.v.	Intravenous(ly)	10
IFN	Interferon	4
IFNAR1	Interferon alpha/beta receptor 1	7
Ifnar1$^{-/-}$	Interferon type I receptor knockout	25
IFNAR2	Interferon alpha/beta receptor 2	7
IFNs	Interferons	7
IFNα	Interferon alpha	7
IFNβ	Interferon beta	7
IFNγ	Interferon gamma	7
IFNλ	Interferon lambda	7
IRF3	Interferon regulatory factor 3	4
IRF7	Interferon regulatory factor 7	4
IVT	*In vitro* transcription	23
LGP2	Laboratory of genetics and physiology 2	4
MACS	Magnetic-activated cell sorting	21
MAVS	Mitochondrial antiviral-signaling protein	4
Mavs$^{-/-}$	Mitochondrial antiviral-signaling protein knockout	25
mCD45+	Murine CD45 positive	48

MDA5	Melanoma differentiation-associated 5	4
MHC-I	Major histocompatibility complex class I	7
MHC-II	Major histocompatibility complex class II	7
mIFNα	murine IFN alpha	40
NF-κB	Nuclear factor kappa-light-chain-enhancer of activated B cells	4
NIH	National Institute of Health	1
NK cell	Natural killer cell	4
NSG	NOD-*scid* IL2Rγ^{null}	19
NTP	Nucleoside triphosphate	24
PAMP	Pathogen-associated molecular pattern	3
panCD45+	Murine CD45 positive plus human CD45 positive cells	48
PBMC	Peripheral blood mononuclear cell	21
PBS	Phosphate buffered saline	14
PD-1	Programmed cell death protein 1	8
PD-L1	Programmed death-ligand 1	8
PDX	Patient-derived xenografted	19
PMMA	Polymethylmethacrylat	27
ppp	Triphosphate	4
ppp-RNA	5'-Triphosphate-RNA	4
PRR	Pattern recognition receptor	3
RIG-I	Retinoic acid-inducible gene I	4
RLR	Retinoic acid-inducible gene-I-like receptor	4
RPMI	Roswell Park Memory Institute	15
SCT	Stem cell transplantation	2
SD	Standard deviation	38
SEM	Standard error of the mean	32
STING	Stimulator of interferon genes	58

TCR	T cell receptor	6
TLR	Toll-like receptor	6
VOI	Viral oncolytic immunotherapy	56
WT	Wild type	30
αPD-1	Anti-PD-1 antibody	26

9. Acknowledgements

10. Affidavit

<table>
<tr><td>LMU
LUDWIG-
MAXIMILIANS-
UNIVERSITÄT
MÜNCHEN</td><td>Promotionsbüro
Medizinische Fakultät</td><td>MMRS</td><td></td></tr>
</table>

Eidesstattliche Versicherung

Ruzicka, Michael
_____
Name, Vorname

Ich erkläre hiermit an Eides statt, dass ich die vorliegende Dissertation mit dem Titel:

Therapeutic RIG-I activation enhances survival and induces sensitivity to immune checkpoint blockade therapy in preclinical models of AML

selbständig verfasst, mich außer der angegebenen keiner weiteren Hilfsmittel bedient und alle Erkenntnisse, die aus dem Schrifttum ganz oder annähernd übernommen sind, als solche kenntlich gemacht und nach ihrer Herkunft unter Bezeichnung der Fundstelle einzeln nachgewiesen habe.

Ich erkläre des Weiteren, dass die hier vorgelegte Dissertation nicht in gleicher oder in ähnlicher Form bei einer anderen Stelle zur Erlangung eines akademischen Grades eingereicht wurde.

München, 25.04.2023   Michael Ruzicka
_____   _____
Ort, Datum   Unterschrift Doktorandin bzw. Doktorand

11. Publications

The results of this work or parts of it were presented and published as an abstract on the following meetings:

1.   **M. Ruzicka**, E. M. Heuer, H. Meinl, L. König, S. Endres, M. Subklewe, F. Lichtenegger, S. Rothenfußer
      Immunotherapy of AML with bifunctional siRNA
      TOLL 2015, Targeting Innate Immunity
      Marbella, Spain

2.   **M. Ruzicka**, E. M. Heuer, H. Meinl, L. König, S. Endres, M. Subklewe, F. Lichtenegger, S. Rothenfußer
      Immunotherapy targeting RIG-I in a mouse model of acute myeloid leukemia
      14th Annual Meeting of the Association for Cancer Immunotherapy, 2016
      Mainz, Germany

3.   **M. Ruzicka**, E. M. Heuer, H. Meinl, L. König, S. Endres, M. Subklewe, F. Lichtenegger, S. Rothenfußer
      Immunotherapy targeting RIG-I in a mouse model of acute myeloid leukemia
      Immunofest 2, 2016
      Munich, Germany

4.   **M. Ruzicka**, L. König, E. M. Heuer, H. Meinl, L. Kocheise, S. Endres, M. Subklewe, F. Lichtenegger, S. Rothenfusser
      Immunotherapy targeting RIG-I in a mouse model of acute myeloid leukemia
      4th Immunotherapy of Cancer Conference, 2017
      Prague, Czech Republic
      Awarded with a poster prize

Parts of this work were published as a scientific article:

1.   **Ruzicka M**, Koenig LM, Formisano S, Boehmer DFR, Vick B, Heuer EM, Meinl H, Kocheise L, Zeitlhöfler M, Ahlfeld J, Kobold S, Endres S, Subklewe M, Duewell P, Schnurr M, Jeremias I, Lichtenegger FS, Rothenfusser S.
     RIG-I-based immunotherapy enhances survival in preclinical AML models and sensitizes AML cells to checkpoint blockade
     Leukemia 2020; 34(4):1017-1026. doi: 10.1038/s41375-019-0639-x.

Further publications by the author:

1.   **Ruzicka M**, Wurm S, Lindner L, Dreyling M, Bergwelt-Baildon M, Boeck S, Giessen-Jung C, Milani V, Stemmler HJ, Subklewe M, Weigert O, Spiekermann K.
     Treatment, outcome and re-vaccination of patients with SARS-CoV-2 vaccine-associated immune thrombocytopenia
     Infection (in press)

2.   Winkelmann M, Bücklein VL, Blumenberg V, Rejeski K, **Ruzicka M**, Unterrainer M, Schmidt C, Dekorsy FJ, Bartenstein P, Ricke J, Bergwelt-Baildon M, Subklewe M, Kunz WG
     Lymphoma tumor burden before chimeric antigen receptor T-Cell treatment: RECIL vs. Lugano vs. metabolic tumor assessment
     Frontiers in Oncology 2022. doi: 10.3389/fonc.2022.974029

3.   Winkelmann M, Rejeski K, Unterrainer M, Schmidt C, **Ruzicka M**, Ricke J, Rudelius M, Subklewe M, Kunz WG.
     Transformation of diffuse large B cell lymphoma into dendritic sarcoma under CAR T cell therapy detected on 18 F-FDG PET/CT
     European Journal of Nuclear Medicine and Molecular Imaging 2021. doi: 10.1007/s00259-020-05000-9

4. Mumm JN, Osterman A, **Ruzicka M**, Stihl C, Vilsmaier T, Munker D, Khatamzas E, Giessen-Jung C, Stief C, Staehler M, Rodler S.
    Urinary Frequency as a Possibly Overlooked Symptom in COVID-19 Patients: Does SARS-CoV-2 Cause Viral Cystitis?
    European Urology 2020; 78(4):624-628. doi: 10.1016/j.eururo.2020.05.013.

5. Unterrainer M, **Ruzicka M**, Fabritius MP, Mittlmeier LM, Winkelmann M, Rübenthaler J, Brendel M, Subklewe M, von Bergwelt-Baildon M, Ricke J, Kunz WG, Cyran CC.
    PET/CT imaging for tumour response assessment to immunotherapy: current status and future directions
    European Radiology Experimental 2020; 17;4(1):63. doi: 10.1186/s41747-020-00190-1.